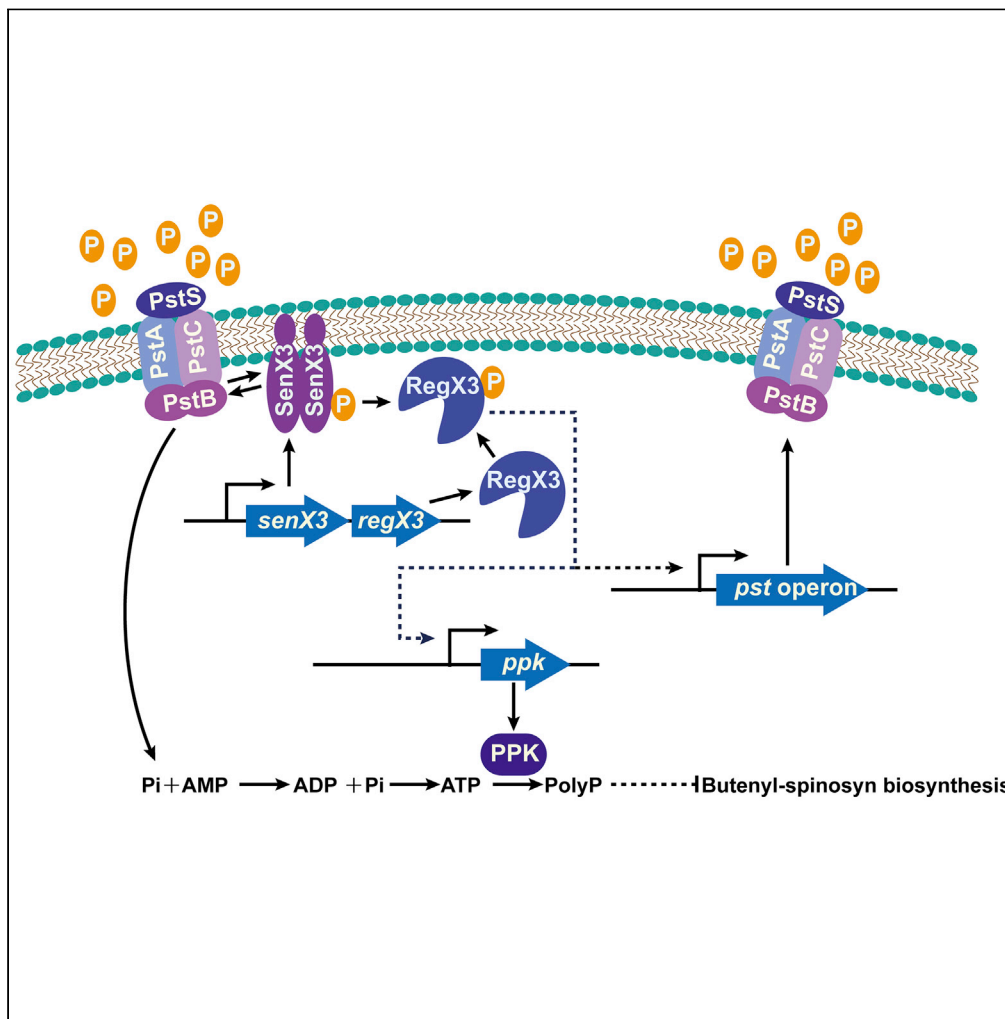# iScience

Article

SenX3-RegX3, an Important Two-Component System, Regulates Strain Growth and Butenyl-spinosyn Biosynthesis in *Saccharopolyspora pogona*

Jie Rang,
Haocheng He,
Jianming Chen, ...,
Xuezhi Ding,
Youming Zhang,
Liqiu Xia

xialq@hunnu.edu.cn

HIGHLIGHTS

Butenyl-spinosyn biosynthesis is highly sensitive to Pi control

RegX3 regulates polyP accumulation in *S. pogona*

RegX3 may indirectly regulate butenyl-spinosyn production

RegX3 plays an important role in the normal growth development of *S. pogona*

Article

SenX3-RegX3, an Important Two-Component System, Regulates Strain Growth and Butenyl-spinosyn Biosynthesis in *Saccharopolyspora pogona*

Jie Rang,[1,2] Haocheng He,[1,2] Jianming Chen,[1] Jinjuan Hu,[1] Jianli Tang,[1] Zhudong Liu,[1] Ziyuan Xia,[1] Xuezhi Ding,[1] Youming Zhang,[1] and Liqiu Xia[1,3,*]

SUMMARY

Butenyl-spinosyn produced by *Saccharopolyspora pogona* exhibits strong insecticidal activity and a broad pesticidal spectrum. Currently, important functional genes involved in butenyl-spinosyn biosynthesis remain unknown, which leads to difficulty in efficient understanding of its regulatory mechanism and improving its production by metabolic engineering. Here, we present data supporting a role of the SenX3-RegX3 system in regulating the butenyl-spinosyn biosynthesis. EMSAs and qRT-PCR demonstrated that RegX3 positively controls butenyl-spinosyn production in an indirect way. Integrated proteomic and metabolomic analysis, *regX3* deletion not only strengthens the basal metabolic ability of *S. pogona* in the mid-growth phase but also promotes the flow of the acetyl-CoA produced via key metabolic pathways into the TCA cycle rather than the butenyl-spinosyn biosynthetic pathway, which ultimately leads to continued growth but reduced butenyl-spinosyn production. The strategy demonstrated here may be valuable for revealing the regulatory role of the SenX3-RegX3 system in the biosynthesis of other natural products.

INTRODUCTION

Butenyl-spinosyn is a secondary metabolite produced by *Saccharopolyspora pogona* (*S. pogona*) (Paul et al., 2009; Huang, et al., 2009). It is known to be an excellent insecticidal agent with good potency and a broad spectrum of activity against a variety of Lepidoptera, Diptera, and Coleoptera and a low level of side effects on the non-target organism. At present, butenyl-spinosyn biosynthetic gene cluster (*bus* cluster) and its biosynthetic pathway have been elaborated (Hahn et al., 2006). In addition, the regulatory mechanism of butenyl-spinosyn biosynthesis has been preliminarily studied. Although no key regulatory genes were found in the 110-kb *bus* cluster, *pnp* and *afsR* were identified outside the *bus* cluster to have significant effects on the butenyl-spinosyn biosynthesis (Li et al., 2018, 2019). Despite these findings, our knowledge of the complex regulatory network underlying butenyl-spinosyn biosynthesis is still limited and fragmentary, which presents an obstacle to rational design of butenyl-spinosyn high-producing strains through metabolic engineering.

The biosynthesis of natural products produced by most actinomycetes is affected by phosphate concentrations in the medium (Romero-Rodríguez et al., 2018; Martín et al., 2012; Solans et al., 2019). Initially, the phosphate effect was attributed to a decrease or inhibition of natural product production as a result of a phosphate increase in the culture medium (Curdová et al., 1976). Further studies on phosphate metabolism-related genes identified several of these genes, such as alkaline phosphatase, polyphosphatase, and low- and high-affinity transporter genes, and the pho regulon (Moura et al., 2001; Vuppada et al., 2018; Santos-Beneit et al., 2008; Martínez-Castro et al., 2018). Additionally, it was found that the molecular mechanism of phosphate control is mainly regulated by a two-component system (Martín et al., 2017).

Currently, there are two kinds of two-component systems known to be involved in phosphate regulation, the PhoR-PhoP system and the SenX3-RegX3 system (Aggarwal et al., 2017; White et al., 2018). The PhoR-PhoP system is conserved in all *Streptomyces* and most other sequenced actinomycetes (Barreiro and Martínez-Castro, 2019). Many studies have demonstrated that this system plays an important regulatory role in cellular differentiation and secondary metabolite biosynthesis in actinomycetes (Sola-Landa et al., 2003,

2005, 2013; Martín et al., 2019). In another system that senses and responds to phosphate, the sensor kinase SenX3 and the response regulator RegX3 were first identified and have been well studied in *Mycobacterium* (Namugenyi et al., 2017; Rifat et al., 2014; Park et al., 2019). In *Mycobacterium smegmatis* (*M. smegmatis*), SenX3-RegX3 has been shown to control the expression of phosphate-dependent genes such as those of the *pstSCAB* and *phnDCE* operons and is required for optimal growth under Pi-limiting conditions (Gebhard and Cook, 2008). Meanwhile, SenX3-RegX3 plays an important role in regulating *M. tuberculosis* membrane vesicle production (White et al., 2018). Despite these characteristics, the function of this system in the regulation of natural product biosynthesis has not been reported. A genomic analysis of *S. pogona* showed that it harbored a complete SenX3-RegX3 system and can be used as a good model for studying the interaction effects between the SenX3-RegX3 system and the regulation of strain growth development and natural product production.

In the present study, we constructed *regX3* deletion and overexpression mutants and investigated the effect of RegX3 on the changes in the strains phenotypes. The *regX3* deletion mutant was used to determine the regulatory mechanism of RegX3-related butenyl-spinosyn biosynthesis at the proteome and metabolome levels and further demonstrated that RegX3 could control target product production by regulating the primary metabolism and the expression of the *bus* cluster. Using electrophoretic mobility shift assays (EMSAs), we found that RegX3 could not bind to the *bus* cluster promoter, suggesting that RegX3 indirectly activates the expression of the *bus* cluster. This work deepens our understanding of butenyl-spinosyn regulatory mechanisms and lays an important foundation for studying the regulatory mechanism of the SenX3-RegX3 system in natural product biosynthesis in other actinomycetes.

RESULTS

Effect of Phosphate on Butenyl-spinosyn Production and Strain Growth

Given the paucity of data regarding the effect of inorganic phosphate (Pi) on *S. pogona* butenyl-spinosyn biosynthesis, we measured its production under the following conditions: Pi-free, low Pi concentration (2.5 μM), and high Pi concentration (4 mM). The results of HPLC, bioassay, and LC-MS/MS confirmed that the chromatographic peak found at 10.67 min was butenyl-spinosyn (Figures 1A, S1, and S2). Next, this chromatographic peak was used as a basis for comparing the butenyl-spinosyn production changes. The results showed that the addition of increasing concentrations of Pi drastically reduced butenyl-spinosyn production in synthetic fermentation medium (SFM) (Figure 1A). Moreover, the promoters that control the expression of polyketide synthase genes (*busA*, *busB*, *busC*, *busD*, *busE*) are subject to phosphate modulation (Figure 1B). Meanwhile, the strain density in the stationary period was decreased under a higher Pi concentration at the same sampling time (Figure 1C). It was demonstrated that butenyl-spinosyn biosynthesis and strain growth are highly sensitive to Pi control.

Since the regulatory mechanism of Pi is controlled by the SenX3-RegX3 system, we are interested in the role of this system in *S. pogona* (Figures S3 and S4). To assess the *in vivo* biological significance of RegX3, we constructed *regX3* deletion and over-expression mutants as well as the complemented strain (Table 1, Figures S5 and S6).

RegX3 Regulates polyP Accumulation via PPK-Dependent *mprAB-sigE-rel* Signaling Cascade in the Intermediate Growth Stage

Inorganic polyphosphate (polyP) is a linear biopolymer of phosphoanhydride-linked phosphate units that is found in all domains of life (Barreiro and Martínez-Castro, 2019). In diverse bacteria, polyP is essential for the stress response, motility, biofilm formation, cell cycle control, natural biosynthesis, and virulence (Esnault et al., 2017; Rao et al., 2009). We examined whether changes in the expression level of the *S. pogona regX3* gene altered polyP storage during fermentation (Figure 2A). It was found that the *S. pogona*-Δ*regX3* and *S. pogona*::*regX3* mutants showed no significant change in polyP accumulation compared with the original strain during early development. However, intracellular polyP was obviously decreased in the *S. pogona*-Δ*regX3* mutant but increased in the *S. pogona*::*regX3* mutant in the intermediate growth stage. The complemented strain *S. pogona*-Δ*regX3*::*regX3* restored the original polyP level, suggesting that *S. pogona* RegX3 can positively regulate polyP accumulation. It has been reported that polyP is synthesized by polyphosphate kinase (PPK) and establishes a PPK-dependent *mprAB-sigE-rel* signaling cascade linking polyP metabolism to the stringent response in *M. tuberculosis* (Liang et al., 2017; Kulakovskaya and Kulaev, 2013; Sureka et al., 2007). The result of qRT-PCR showed that the transcriptional level of *ppk* was significantly downregulated in the *S. pogona*-Δ*regX3* mutant, whereas the opposite
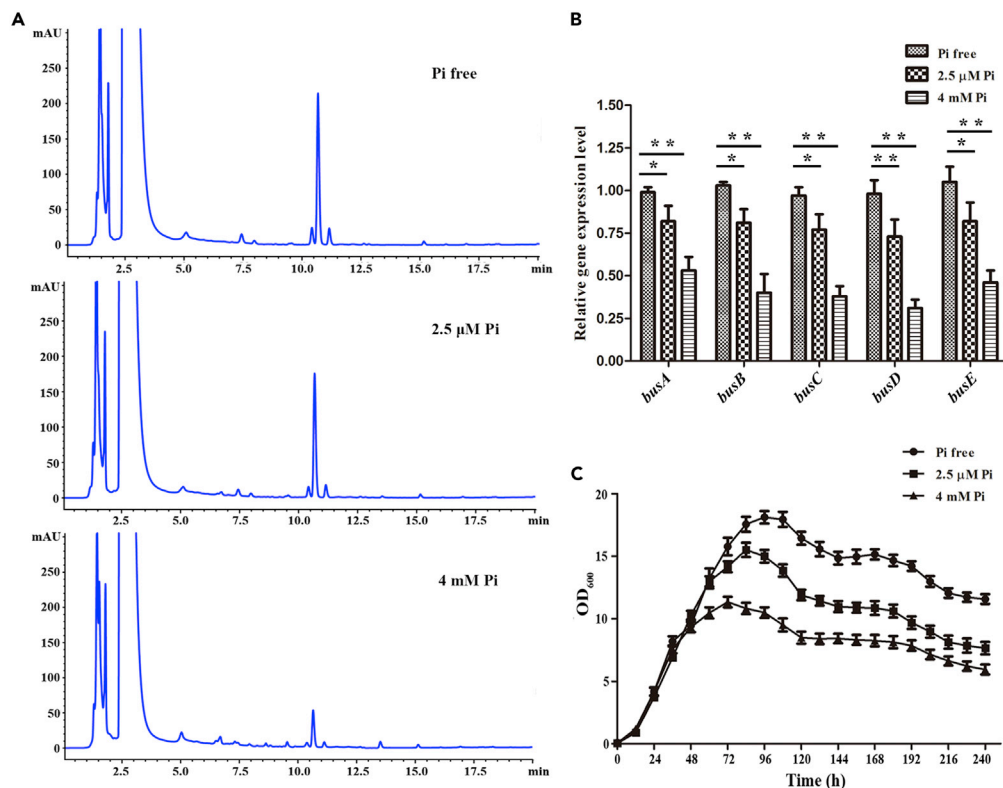
Figure 1. Effect of Phosphate on Butenyl-Spinosyn Production and Strain Growth

(A) Effect of increasing Pi concentrations (0, 2.5×10^{-3}, and 4 mM) on butenyl-spinosyn production.

(B) Effect of increasing Pi concentrations (0, 2.5×10^{-3}, and 4 mM) on the gene expression of butenyl-spinosyn polyketide synthases. *S. pogona* was inoculated into SFM with different Pi concentrations and cultured at 30°C for 4 days. Total RNA was then isolated and used for qRT-PCR assays. The control was free Pi. The 16S rRNA served as the normalization control (**$p < 0.01$; *$p < 0.05$; n = 4).

(C) Effect of increasing Pi concentrations (0, 2.5×10^{-3}, and 4 mM) on strain growth.

pattern was observed in the *S. pogona::regX3* mutant, indicating that RegX3 also regulates polyP accumulation by the PPK-dependent *mprAB-sigE-rel* signaling cascade in *S. pogona* (Figure 2B).

Effects of RegX3 Expression Abundance Changes on *S. pogona* Butenyl-spinosyn Biosynthesis and Other Physiological and Biochemical Characteristics

To determine the roles of RegX3 in butenyl-spinosyn biosynthesis, HPLC was used to estimate butenyl-spinosyn production by the *S. pogona-ΔregX3* and *S. pogona::regX3* mutants. The peak areas of butenyl-spinosyn in the original strain and the *S. pogona-ΔregX3* and *S. pogona::regX3* mutants were 1,084.3 ± 72.37, 305.87 ± 32.02, and 682.57 ± 58.60 mAU*s, respectively (Figures 3A–3C). Meanwhile, the complemented strain *S. pogona-ΔregX3::regX3* restored the original butenyl-spinosyn level (Figure S7). Therefore, *regX3* deletion significantly decreased the production of butenyl-spinosyn by 71.8% compared with that in the original strain. Surprisingly, *regX3* overexpression also decreased the production of butenyl-spinosyn by 37.05% compared with that in the original strain. The above polyP analysis results showed that the overexpression of *regX3* greatly promoted the absorption of extracellular Pi by *S. pogona* and resulted in polyP overproduction, which may be an important reason for the decrease in butenyl-spinosyn production. To confirm this hypothesis, we estimated the butenyl-spinosyn production of the *S. pogona::regX3* mutant in the SFM without Pi and found that its production was increased by 230% compared with that in SFM (Figure 3D). Moreover, the qRT-PCR results showed that *regX3* deletion resulted in a significant decrease in the expression of *busA*, *busF*, *busG*, and *busI* (Figures 3E and 3F). As expected, *regX3* overexpression in SFM also led to the downregulation of the expression of these genes, but the expression of *busA*, *busF*, *busG*, and *busI* was significantly upregulated in the SFM without Pi. To examine whether phosphorylated RegX3 might directly regulate transcription of the *bus* cluster, His₆SenX3 and His₆RegX3 were expressed in *E. coli*

Strains/Plasmids	Description	Source
S. pogona		
NRRL 30141	*S. pogona*, wild-type strain, plasmid-free parental strain	This lab
S. pogona-ΔregX3	*S. pogona*, *regX3* deletion strain	This work
S. pogona::regX3	*S. pogona*, *regX3* over-expressed strain	This work
S. pogona-ΔregX3::regX3	*S. pogona-ΔregX3*, *regX3* complemented strain	This work
E. coli		
DH5α	*Escherichia coli*, plasmid-free, host for general cloning	This lab
BL21	*Escherichia coli*, plasmid-free, host for heterologous protein expression	This lab
Plasmids		
pOJ260	*E. coli*-cloning vector, containing pUC18 replicon, *oriT*, Apr^R	This lab
pKC-*tsr*	acc(3)IV, pSG5, j23119, vector for expression	This lab
pOJ260-cm-PermE	pOJ260 containing *PermE*, for *PermE* PCR amplification	This lab
pOJ260-UA$_{regX3}$-apr-DA$_{regX3}$	pOJ260 containing homologous region flanking *regX3*, for *regX3* deletion	This work
pOJ260-PermE-regX3	pOJ260 containing *PermE* and *regX3*, for *regX3* overexpression	This work
pKC-tsr-regX3	pKC-*tsr* containing *regX3*, for *regX3* complementation	This work

Table 1. Strains and Plasmids in This Study

BL21, and their affinity toward the three regions containing *bus* promoters was examined in EMSAs (Figure 3G). The results showed that RegX3 did not bind to the *bus* promoters, demonstrating that RegX3 may regulate butenyl-spinosyn production by indirectly promoting the expression of the *bus* cluster (Figure 3H).

For other physiological and biochemical characteristics, the *S. pogona-ΔregX3* mutant exhibited a slower growth rate and glucose consumption rate compared with the original strain during the test period (Figure 4). However, the *S. pogona::regX3* mutant also showed inhibited strain growth and glucose consumption, and its inhibition was slightly greater than that of the *S. pogona-ΔregX3* mutant, indicating that RegX3 plays an important role in maintaining the normal growth development of *S. pogona*.

Overview of the Comparative Proteomic and Targeted Metabolomic Analysis

To explain why *regX3* deletion causes the above phenomenon, we further carried out a comparative proteomics analysis using iTRAQ labeling in the *S. pogona-ΔregX3* mutant. According to the butenyl-spinosyn production analysis, the butenyl-spinosyn production of the *S. pogona-ΔregX3* mutant began to stabilize on day 6 (Figure S8). This time point was selected for protein extraction from the *S. pogona-ΔregX3* mutant and original strain separately. The resulting mass spectra were searched against the *S. pogona* proteome database, and a total of 2,533 proteins were identified (unique peptides >1) (Data S1, Figure 5A). Using a 1.33-fold cutoff, there were 128 proteins differentially expressed between the *S. pogona-ΔregX3* mutant and original strain (Data S2, Figure 5B). These differentially expressed proteins were involved in multiple biological processes, such as glycolysis, pentose phosphate pathway (PP pathway), TCA cycle, fatty acid metabolism, oxidative phosphorylation, amino acid metabolism, two-component system, and ABC transporters, which suggests that RegX3 is likely to be a global regulator.

To analyze whether the changes in metabolite abundance related to strain growth and target product biosynthesis were consistent with the changes in proteins, the intracellular metabolome was evaluated by LC-MS/MS. The samples from day 6 were also used for metabolomic profiling to analyze the correlation with the proteomic data. As a result, 21 intracellular metabolites were identified and quantified by LC-MS/MS, which are mainly involved in glycolysis, PP pathway, TCA cycle, and oxidative phosphorylation (Table 2, Data S3).
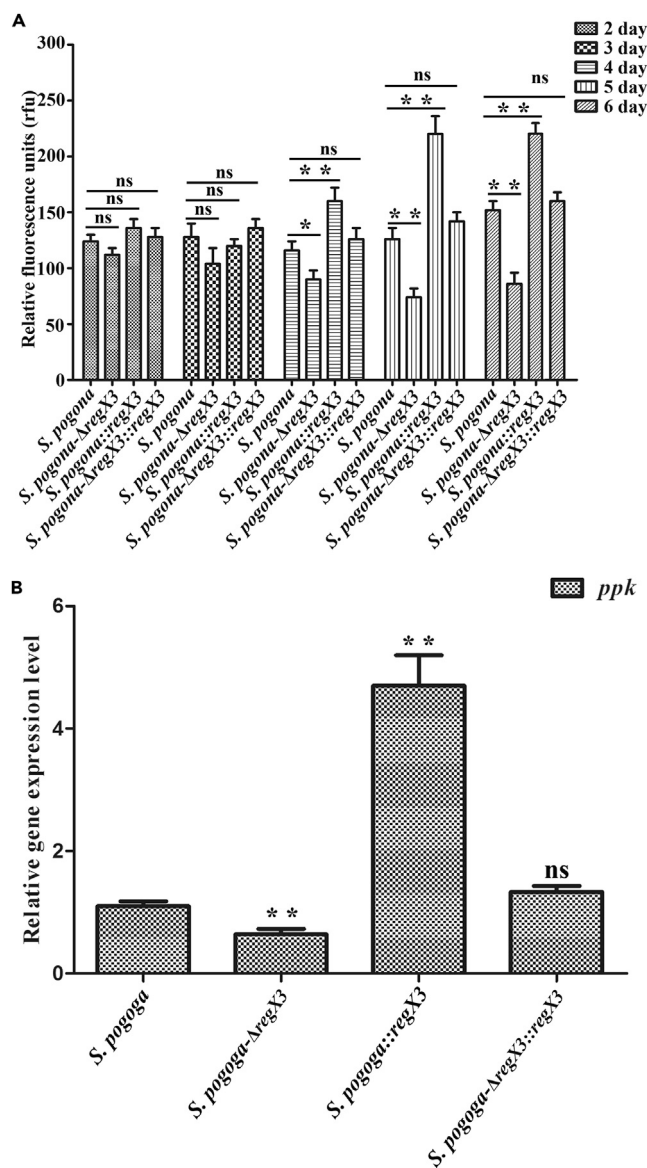
Figure 2. Effect of *regX3* Deletion and Overexpression on Polyphosphate (polyP) Accumulation

(A) Comparative analysis of polyP accumulation in different strains. Wild-type *S. pogona*, *S. pogona*-Δ*regX*, and *S. pogona*::*regX3* mutants and complemented strain *S. pogona*-Δ*regX*::*regX3* were inoculated into SFM at equal OD_{600} values and grown at 30°C. Cells in the early and intermediate stages of growth were collected, and their polyP contents were determined via the DAPI method. The data shown are the mean values ± standard deviations of three independent experiments (**$p < 0.01$; *$p < 0.05$; ns, no significance; n = 3).

(B) The *ppk* transcript was measured in different strains. The cells of the different strains were inoculated into SFM and cultured at 30°C for 4 days. Total RNA was then isolated and used for qRT-PCR assays. The control strain was wild-type *S. pogona*. 16S rRNA served as the normalization control (**$p < 0.01$; ns, no significance; n = 4).

RegX3 Deletion Leads to an Increased Acetyl-CoA Metabolic Flux to the TCA Cycle

The current study provides an overview of the central carbon metabolic pathway and the changes in the expression levels of proteins and metabolites involved in key metabolic pathways, as shown in Figure 6. Most enzymes and their catalytic products involved in central carbon metabolism could be identified from the shotgun proteomic and targeted metabolomic data. PTS glucose transporter IIA (PTS IIA) was identified, and its abundance in the *S. pogona*-Δ*regX3* mutant was higher than that in the original strain. As shown in the metabolomic analysis, glucose 6-phosphate presented higher abundance in the

S. pogona-Δ*regX3* mutant, indicating that the ability of the *S. pogona*-Δ*regX3* mutant to transport and phosphorylate glucose was stronger than that of the original strain, which was consistent with the rapid glucose consumption rate and the improvement of cell growth.

Glycolysis and the PP pathway are two main mechanisms whereby microorganisms metabolize glucose (Seol et al., 2016; Nikel et al., 2015). Throughout glycolysis, the abundance of 6-phosphofructokinase (*pfkA*), which is a rate-limiting enzyme for glycolysis, and its catalytic product fructose 1,6-diphosphate in the *S. pogona*-Δ*regX3* mutant was higher than that in the original strain. However, other enzymes (phosphoglycerate mutase [*gpmA*], enolase [*eno*], and pyruvate dehydrogenase [*aceE*, *bkdC1*]) and metabolites (phosphoenolpyruvate and pyruvate) involved in glycolysis, their abundance in the *S. pogona*-Δ*regX3* mutant was opposite. The PP pathway is the second most important pathway for glucose metabolism, and its initial substrate is glucose 6-phosphate (Nikel et al., 2015). We found that no differentially expressed proteins related to the oxidative branch of the PP pathway were detectable in the *S. pogona*-Δ*regX3* mutant. Interestingly, differentially expressed proteins (transketolase [*tktA2*], transaldolase [*tal*], and ribulose-phosphate 3-epimerase [*rpe*]) and fructose 6-phosphate related to the non-oxidative branch of the PP pathway were identified in the *S. pogona*-Δ*regX3* mutant, and their abundance was significantly higher than in the original strain. In addition, ribose-phosphate pyrophosphokinase (*prsA*) was identified in our proteomic data, which is one of the rate-limiting enzymes of purine metabolism, and its abundance was also higher than in the original strain. The above detection results suggest that *regX3* inactivation can improve the abilities of glycolysis, compounds with different carbon numbers to undergo mutual conversion and synthesize ATP, GTP, and their derivatives, but inhibit the generation of acetyl-CoA from pyruvate.

Fatty acid degradation metabolism is an important metabolic pathway for the synthesis of acetyl-CoA (Kallscheuer et al., 2017). The proteomic data obtained in the present study showed that the abundance of enoyl-CoA hydratase (*echA*), 3-hydroxybutyryl-CoA dehydrogenase (*fadB*), and acetyl-CoA acyltransferase (*fadA*, *catF*) in the *S. pogona*-Δ*regX3* mutant was higher than that in the original strain. These data indicate that RegX3 inactivation increased the degradation ability of fatty acid. The acetyl-CoA produced through glycolysis and fatty acid degradation metabolism will enter the TCA cycle to produce energy and several metabolic precursors for cell growth and the synthesis of other metabolites (Vuoristo et al., 2017). Citrate synthase (*citA*), isocitrate dehydrogenase (*icd-2*), and 2-oxoglutarate dehydrogenase (*sucB*) are the rate-limiting enzymes of the TCA cycle and were detected in our proteomic data. The abundance of these three rate-limiting enzymes and other enzymes involved in the TCA cycle, such as aconitate hydratase (*acn*), succinyl-CoA synthetase (*sucC*, *sucD*), fumarate reductase (*fumA*), and malate dehydrogenase (*mdh*), in the *S. pogona*-Δ*regX3* mutant was higher than that in the original strain. Additionally, citrate, 2-oxoglutarate, succinate, and malate exhibited higher abundance in the *S. pogona*-Δ*regX3* mutant, although the abundance of succinate dehydrogenase (*sdhA*) and its catalytic product fumarate was low. These data suggest that the *S. pogona*-Δ*regX3* mutant shows a greater metabolic capacity than the original strain in terms of central carbon metabolism, so it can continue to absorb and utilize nutrients in the extracellular environment during the analysis phase. Moreover, the metabolic flux flowing through the TCA cycle in the *S. pogona*-Δ*regX3* mutant is increased compared with that in the original strain, which may increase the flow of the acetyl-CoA produced via glycolysis, fatty acid degradation, and other metabolic pathways into the TCA cycle and ultimately limits butenyl-spinosyn biosynthesis.

DISCUSSION

The effect of inorganic phosphate on the physiology and antibiotic production of most actinomycetes has been known for some time (Romero-Rodríguez et al., 2018; Barreiro and Martínez-Castro, 2019). In general, it has been observed that high phosphate concentrations in the culture medium stimulate strain growth and inhibit natural product biosynthesis, as occurs in *S. filipinensis* (filipin), *S. avermitilis* (avermectin), and *S. clavuligerus* (clavulanic acid) (Martín et al., 2017; Barreales et al., 2018). In our study, phosphate also affects growth development and butenyl-spinosyn biosynthesis in *S. pogona*. Three phosphate systems with different concentrations (0, 2.5×10^{-3}, and 4 mM) were established in this study; however, the bacterial density and target product production in the medium without phosphate were significantly higher than those in the low-phosphate concentration and high-phosphate concentration systems. These results demonstrate that butenyl-spinosyn production is also highly sensitive to phosphate control, in contrast to the lower sensitivity of other classes of secondary metabolites, such as orthosomycin antibiotics (Zhu et al.,
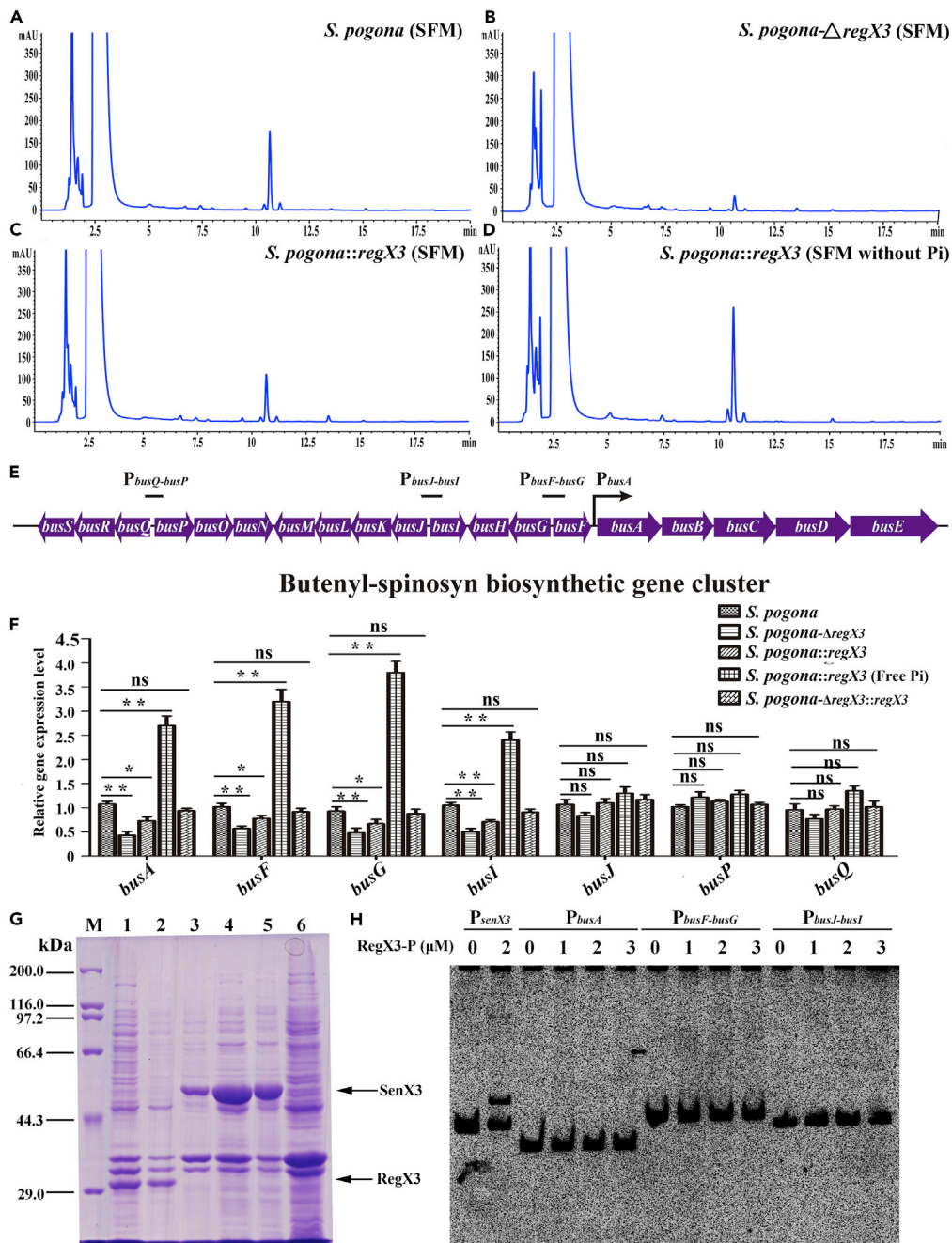
Figure 3. RegX3 Positively Regulates Butenyl-Spinosyn Production in *S. pogona*

(A–C) Comparison of butenyl-spinosyn production in wild-type *S. pogona* and the *S. pogona*-Δ*regX* and *S. pogona*::*regX3* mutants in SFM via HPLC analysis.

(C and D) Comparison of butenyl-spinosyn production in the *S. pogona*::*regX3* mutant in SFM and SFM without Pi via HPLC analysis.

(E) Genetic organization of the *bus* cluster in *S. pogona*.

(F) Effect of *regX3* deletion and overexpression on the transcription level of *bus* cluster in SFM or SFM without Pi. The cells of the different strains were inoculated into SFM or SFM without Pi and cultured at 30°C for 4 days. Total RNA was then isolated and used for qRT-PCR assays. The control strain was wild-type *S. pogona*. 16S rRNA served as the normalization control (**p < 0.01; *p < 0.05; ns, no significance; n = 4).

(G) Heterologous expression of *regX3* and *senX3*. Lane M, protein marker; lane 1 and 2, heterologous expression of *regX3* in *E. coli* BL21; lane 3–5, heterologous expression of *senX3* in *E. coli* BL21; lane 6, *E. coli* BL21 (Control).

(H) EMSAs assessing the interaction of the P$_{busA}$, P$_{busF-busG}$, and P$_{busJ-busI}$ probes with the purified His$_6$-tagged RegX3-P protein.
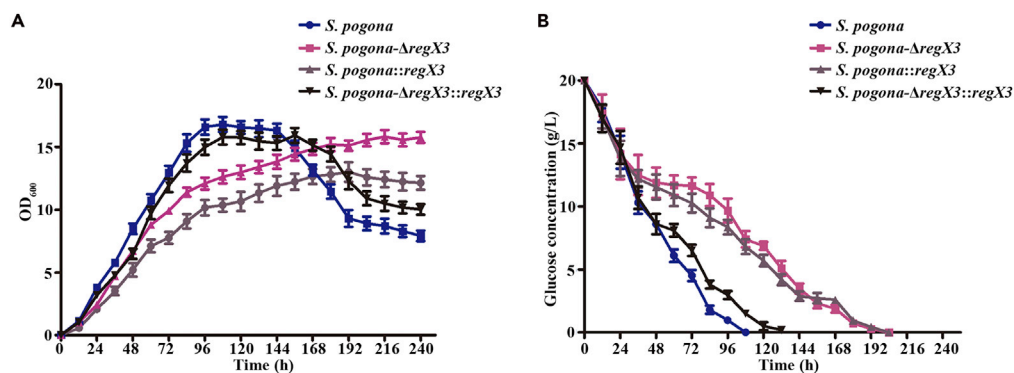
Figure 4. Effect of *regX3* Deletion and Overexpression on Strain Growth Kinetics and Glucose Consumption
(A) Growth kinetics analysis of wild-type *S. pogona* and its derivatives in SFM.
(B) Comparison of glucose utilization in wild-type *S. pogona* and its derivatives in SFM.

2007) or cephalosporins (Leite et al., 2016), that are only inhibited at high phosphate concentrations (20–100 mM).

Recent studies have shown that the absorption and assimilation of extracellular phosphate by actinomycetes is related to the regulation of the intracellular Pho regulon, whereas the pho regulon is usually controlled by two-component systems (Sola-Landa et al., 2013; Allenby et al., 2012; Glover et al., 2007). PhoR-PhoP and SenX3-RegX3 are two classes of two-component systems associated with phosphate regulation. Although the PhoR-PhoP and SenX3-RegX3 systems are related to phosphate regulation, only the PhoR-PhoP system has been reported in Streptomyces, and it negatively regulates the biosynthesis of most natural products (Sola-Landa et al., 2003; Barreiro and Martínez-Castro, 2019; Yang et al., 2015; Mendes et al., 2007). The analysis of sequenced *Streptomyces* genomes showed that most *Streptomyces* do not contain the *senX3-regX3* system, with the exception of *S. coelicolor*, *S. griseoruber*, and *S. davaonensis*. Therefore, no research on the regulatory mechanism of the SenX3-RegX3 system related to natural product biosynthesis has been reported. However, the SenX3-RegX3 system is found in the genomes of various *Mycobacterial* species, indicating that this evolutionarily conserved two-component system may play a fundamental regulatory role in *Mycobacterial* physiology, such as bacterial survival and chronic infections in mouse lungs (Rifat et al., 2014; James et al., 2012). The genomic analysis of *S. pogona* showed that it exhibited a complete *senX3-regX3* system and the organization of *senX3-regX3* and the adjacent gene *gpmA* and *ppx-gppA* was the same as in the homologous region in *M. smegmatis*, suggesting that the *senX3-regX3* system in *S. pogona* may present similar transcription patterns and biological functions to those of *M. smegmatis* (Figure S9). Pi has an important influence on strain growth and natural product biosynthesis, and its regulatory mechanism can be controlled by the SenX3-RegX3 system (Glover et al., 2007). Therefore, this system is likely to exhibit a special relationship with the normal growth development and butenyl-spinosyn biosynthesis of *S. pogona*.

In this work, the inactivation of *regX3* obviously decreased the production of butenyl-spinosyn by 71.8%. Moreover, the expression levels of some *bus* genes in the *S. pogona*-Δ*regX3* mutant were significantly downregulated compared with those in the original strain. EMSA showed that the SenX3-RegX3 system regulates butenyl-spinosyn biosynthesis by indirectly promoting the expression of the *bus* cluster. These data suggest that RegX3 may act as a pleiotropic regulator to control butenyl-spinosyn biosynthesis. Proteomic and targeted metabolomic analyses were first used to compare the *S. pogona*-Δ*regX3* mutant and original strain. A total of 55 proteins and 10 metabolites were found to be upregulated, whereas 63 proteins and 6 metabolites were downregulated in the *S. pogona*-Δ*regX3* mutant. These differentially expressed proteins are involved in multiple biological processes such as glycolysis, PP pathway, TCA cycle, fatty acid metabolism, oxidative phosphorylation, amino acid metabolism, two-component system, and ABC transporters, which further explains the regulatory characteristics of RegX3.
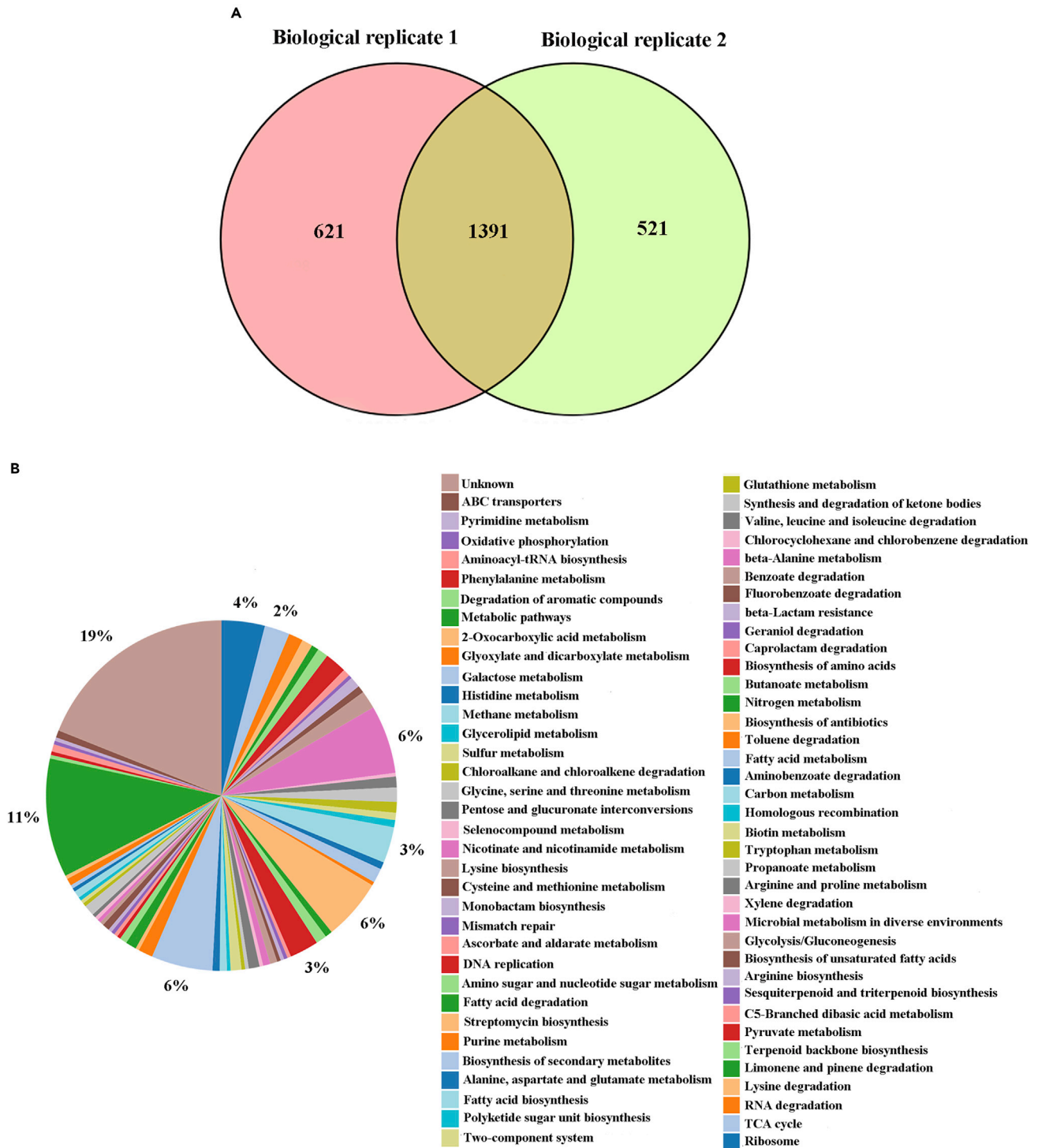
Figure 5. Comparative Proteomic Analysis between the *S. pogona-ΔregX* Mutant and Wild-Type *S. pogona*.
(A) Venn diagram of protein identification in two biological replicates. The number of proteins is shown in each area.
(B) KEGG pathway analysis of differentially expressed proteins.

Metabolites	KEGG Pathway	Fold change (*S. pogona-ΔregX3/S. pogona*)	p Value
Succinate	TCA cycle	2.813	0.002
Beta-D-Fructose 6-phosphate	Glycolysis	2.492	0.017
NADH	Oxidative phosphorylation	2.093	0.001
L-Malic acid	TCA cycle	1.932	0.018
D-Glucose 6-phosphate	Glycolysis	1.741	0.014
NAD	Oxidative phosphorylation	1.685	0.011
Citrate	TCA cycle	1.678	0.004
Alpha-ketoglutarate	TCA cycle	1.595	0.030
NADP	Pentose-phosphate pathway	1.526	0.043
Pyruvate	Glycolysis	0.410	0.004
Lactate	Glycolysis	0.258	0.025
Fumarate	TCA cycle	0.249	0.026
AMP	Oxidative phosphorylation	0.169	0.006
Phosphoenolpyruvate	Glycolysis	0.101	0.004
FMN	Oxidative phosphorylation	0.098	0.004

Table 2. *regX3* Deletion Resulted in Differential Expression of Metabolites Related to Energy Metabolism

Acetyl-CoA, malonyl-CoA, methylmalonyl-CoA, rhamnose, forosamine, and S-adenosyl methionine are important precursors for butenyl-spinosyn biosynthesis (Huang et al., 2009), which are mainly produced through primary metabolic activities. The proteome and metabolome data allowed the identification of most proteins and metabolites involved in the primary metabolism, among which the upregulated proteins not only promote the conversion of extracellular glucose to phosphorylated glucose but also enhance the fatty acid degradation ability and the nonoxidative PP pathway, which provides sufficient precursors for other biological processes. The TCA cycle is a central pathway for the metabolism of carbon sources, lipids, and amino acids and represents a major energy source for cells (Vuoristo et al., 2017). In the *S. pogona-ΔregX3* mutant, most proteins involved in the TCA cycle are upregulated, including aconitate hydratase, isocitrate dehydrogenase, 2-oxoglutarate dehydrogenase, succinyl-CoA synthetase, fumarate reductase, and malate dehydrogenase. Therefore, the proportion of acetyl-CoA produced through glycolysis, fatty acid degradation, and other metabolic activities entering the TCA cycle is increased, whereas the amount of acetyl-CoA utilized for butenyl-spinosyn biosynthesis is reduced. These results may explain why the *S. pogona-ΔregX3* mutant exhibited low butenyl-spinosyn production and increased biomass.

In conclusion, we have shown that the SenX3-RegX3 system plays a very important role in the regulation of growth development and butenyl-spinosyn biosynthesis in *S. pogona*. Our present findings provide a strategy for the improvement of butenyl-spinosyn production based on the engineering of *regX3*. Although multiple differentially expressed proteins affected by RegX3 were identified based on comparative proteomic analysis, the detailed regulatory mechanism is not clear. Therefore, chromatin immunoprecipitation sequencing (ChIP-seq) analysis and *in vitro* characterization of RegX3 targets will be useful for further clarifying the regulatory role of RegX3 in butenyl-spinosyn biosynthesis in *S. pogona*.

Limitations of the Study

In this study, we provide a systematic perspective to demonstrate the SenX3/RegX3 system can control the normal growth development and butenyl-spinosyn biosynthesis of *S. pogona*, laying an important foundation for revealing the butenyl-spinosyn biosynthetic regulatory mechanism. The limitation of this study is

Figure 6. Effect of *regX3* Deletion on Primary Metabolism in *S. pogona*.
This regulatory network is based on the analysis of differentially expressed proteins and metabolites associated with glucose transport, glycolysis, the pentose phosphate pathway, the TCA cycle, and fatty acid degradation. Reactions are reported according to KEGG metabolic pathway databases. Triangle represents a change in protein abundance, and arrow represents a change in metabolite abundance.

that we have not definitively identified the target genes regulated by RegX3, although several differentially expressed proteins were found based on proteomic data. In addition, the relationship among phosphate concentration, SenX3/RegX3 system, and butenyl-spinosyn biosynthesis needs to be analyzed in depth. Additional experiments such as ChIP-seq and EMSAs are needed to further reveal the biological function of SenX3/RegX3 system.

Resource Availability

Lead Contact

Further information and requests for resources should be directed to and will be fulfilled by the Lead Contact, Liqiu Xia (xialq@hunnu.edu.cn).

Materials Availability

This study did not generate new materials.

Data and Code Availability

In the Supplemental Information, we have provided all the required data needed for reproducibility of this work.

Methods

All methods can be found in the accompanying Transparent Methods supplemental file. The strains, plasmids, and primers used in this study are listed in Tables S1 and S2, respectively.

SUPPLEMENTAL INFORMATION

Supplemental Information can be found online at https://doi.org/10.1016/j.isci.2020.101398.

AUTHOR CONTRIBUTIONS

L.X. conceived the project. L.X., Y.Z., and J.R. generated ideas and designed research. J.R., H.H., and J.T. performed iTraq-based quantitative proteomic and targeted metabolomic samples preparation and bioinformatics analysis. J.R., H.H., J.H., J.C., and Z.L. performed the mutants construction, RegX3 heterologous expression, and EMSAs assays. J.R., X.D., J.T., H.H., and Z.X. performed butenyl-spinosyn HPLC and MS analysis. J.R., H.H., J.H., and J.C. performed mutant strains physiological and biochemical assay. J.R. and L.X. wrote the manuscript. All authors discussed the results and approved the final manuscript.

DECLARATION OF INTERESTS

The authors declare that they have no conflicts of interest.

REFERENCES

Aggarwal, S., Somani, V.K., Gupta, V., Kaur, J., Singh, D., Grover, A., and Bhatnagar, R. (2017). Functional characterization of PhoPR two component system and its implication in regulating phosphate homeostasis in *Bacillus anthracis*. Biochim. Biophys. Acta Gen. Subj. *1861* (1 Pt A), 2956–2970.

Allenby, N.E., Laing, E., Bucca, G., Kierzek, A.M., and Smith, C.P. (2012). Diverse control of metabolism and other cellular processes in *Streptomyces coelicolor* by the PhoP transcription factor: genome-wide identification of in vivo targets. Nucleic Acids Res. *40*, 9543–9556.

Barreales, E.G., Payero, T.D., de Pedro, A., and Aparicio, J.F. (2018). Phosphate effect on filipin production and morphological differentiation in *Streptomyces filipinensis* and the role of the PhoP transcription factor. PLoS One *13*, e0208278.

Barreiro, C., and Martínez-Castro, M. (2019). Regulation of the phosphate metabolism in *Streptomyces* genus: impact on the secondary metabolites. Appl. Microbiol. Biotechnol. *103*, 1643–1658.

Curdová, E., Kremen, A., Vaněk, Z., and Hostálek, Z. (1976). Regulation and biosynthesis of secondary metabolites. XVIII. Adenylate level and chlorotetracycline production in *Streptomyces aureofaciens*. Folia. Microbiol. (Praha) *21*, 481–487.

Esnault, C., Dulermo, T., Smirnov, A., Askora, A., David, M., Deniset-Besseau, A., Holland, I.B., and Virolle, M.J. (2017). Strong antibiotic production

is correlated with highly active oxidative metabolism in *Streptomyces coelicolor* M145. Sci. Rep. *7*, 200.

Gebhard, S., and Cook, G.M. (2008). Differential regulation of high-affinity phosphate transport systems of *Mycobacterium smegmatis*: identification of PhnF, a repressor of the *phnDCE* operon. J. Bacteriol. *190*, 1335–1343.

Glover, R.T., Kriakov, J., Garforth, S.J., Baughn, A.D., and Jacobs, W.R., Jr. (2007). The two-component regulatory system *senX3-regX3* regulates phosphate-dependent gene expression in *Mycobacterium smegmatis*. J. Bacteriol. *189*, 5495–5503.

Hahn, D.R., Gustafson, G., Waldron, C., Bullard, B., Jackson, J.D., and Mitchell, J. (2006). Butenyl-spinosyns, a natural example of genetic engineering of antibiotic biosynthetic genes. J. Ind. Microbiol. Biotechnol. *33*, 94–104.

Huang, K.X., Xia, L.Q., Zhang, Y.M., Ding, X.Z., and Zahn, J.A. (2009). Recent advances in the biochemistry of spinosyns. Appl. Microbiol. Biotechnol. *82*, 13–23.

James, J.N., Hasan, Z.U., Ioerger, T.R., Brown, A.C., Personne, Y., Carroll, P., Ikeh, M., Tilston-Lunel, N.L., Palavecino, C., Sacchettini, J.C., and Parish, T. (2012). Deletion of SenX3-RegX3, a key two-component regulatory system of *Mycobacterium smegmatis*, results in growth defects under phosphate-limiting conditions. Microbiology *158* (Pt 11), 2724–2731.

Kallscheuer, N., Polen, T., Bott, M., and Marienhagen, J. (2017). Reversal of β-oxidative pathways for the microbial production of chemicals and polymer building blocks. Metab. Eng. *42*, 33–42.

Kulakovskaya, T., and Kulaev, I. (2013). Enzymes of inorganic polyphosphate metabolism. Prog. Mol. Subcell. Biol. *54*, 39–63.

Leite, C.A., Cavallieri, A.P., Baptista, A.S., and Araujo, M.L. (2016). Dissociation of cephamycin C and clavulanic acid biosynthesis by 1,3-diaminopropane in *Streptomyces clavuligerus*. FEMS Microbiol. Lett. *363*, fnv215.

Li, L., Rang, J., He, H.C., He, S.Y., Liu, Z.D., Tang, J.L., Xiao, J., He, L., Hu, S.B., Yu, Z.Q., et al. (2018). Impact on strain growth and butenyl-spinosyn biosynthesis by overexpression of polynucleotide phosphorylase gene in *Saccharopolyspora pogona*. Appl. Microbiol. Biotechnol. *102*, 8011–8021.

Li, L., Gong, L., He, H.C., Liu, Z.D., Rang, J., Tang, J.L., Peng, S.N., Yuan, S.Q., Ding, X.Z., Yu, Z.Q., et al. (2019). AfsR is an important regulatory factor for growth and butenyl-spinosyn biosynthesis of *Saccharopolyspora pogona*. Ann. Microbiol. *69*, 809–818.

Martín, J.F., Santos-Beneit, F., Rodríguez-García, A., Sola-Landa, A., Smith, M.C., Ellingsen, T.E., Nieselt, K., Burroughs, N.J., and Wellington, E.M. (2012). Transcriptomic studies of phosphate control of primary and secondary metabolism in *Streptomyces coelicolor*. Appl. Microbiol. Biotechnol. *95*, 61–75.

Martín, J.F., Rodríguez-García, A., and Liras, P. (2017). The master regulator PhoP coordinates phosphate and nitrogen metabolism, respiration,

cell differentiation and antibiotic biosynthesis: comparison in *Streptomyces coelicolor* and *Streptomyces avermitilis*. J. Antibiot. (Tokyo). *70*, 534–541.

Liang, M., Frank, S., Lünsdorf, H., Warren, M.J., and Prentice, M.B. (2017). Bacterial microcompartment-directed polyphosphate kinase promotes stable polyphosphate accumulation in *E. coli*. Biotechnol. J. *12*, 10.

Martín, J.F., Ramos, A., and Liras, P. (2019). Regulation of geldanamycin biosynthesis by cluster-situated transcription factors and the master regulator PhoP. Antibiotics (Basel) *8*, E87.

Martínez-Castro, M., Barreiro, C., and Martín, J.F. (2018). Analysis and validation of the pho regulon in the tacrolimus-producer strain *Streptomyces tsukubaensis*: differences with the model organism *Streptomyces coelicolor*. Appl. Microbiol. Biotechnol. *102*, 7029–7045.

Mendes, M.V., Tunca, S., Antón, N., Recio, E., Sola-Landa, A., Aparicio, J.F., and Martín, J.F. (2007). The two-component *phoR-phoP* system of *Streptomyces natalensis*: inactivation or deletion of *phoP* reduces the negative phosphate regulation of pimaricin biosynthesis. Metab. Eng. *9*, 217–227.

Moura, R.S., Martín, J.F., Martín, A., and Liras, P. (2001). Substrate analysis and molecular cloning of the extracellular alkaline phosphatase of *Streptomyces griseus*. Microbiology *147* (Pt 6), 1525–1533.

Namugenyi, S.B., Aagesen, A.M., Elliott, S.R., and Tischler, A.D. (2017). *Mycobacterium tuberculosis* PhoY proteins promote persister formation by mediating Pst/SenX3-RegX3 phosphate sensing. MBio *8*, e00494-17.

Nikel, P.I., Chavarría, M., Fuhrer, T., Sauer, U., and de Lorenzo, V. (2015). *Pseudomonas putida* KT2440 strain metabolizes glucose through a cycle formed by enzymes of the Entner-Doudoroff, Embden-Meyerhof-Parnas, and Pentose Phosphate Pathways. J. Biol. Chem. *290*, 25920–25932.

Park, E.J., Kwon, Y.M., Lee, J.W., Kang, H.Y., and Oh, J.I. (2019). Dual control of RegX3 transcriptional activity by SenX3 and PknB. J. Biol. Chem. *294*, 11023–11034.

Paul, L., Hahn, D.R., Karr, L.L., Duebelbeis, D.O., Gilbert, J.R., Crouse, G.D., Thomas, W., Thomas, C.S., Pat, M.R.E., and Paul, R.G. (2009). Discovery of the butenyl-spinosyn insecticides: novel macrolides from the new bacterial strain *Saccharopolyspora pogona*. Bioorg. Med. Chem. *17*, 4185–4196.

Rao, N.N., Gómez-García, M.R., and Kornberg, A. (2009). Inorganic polyphosphate: essential for growth and survival. Annu. Rev. Biochem. *78*, 605–647.

Rifat, D., Belchis, D.A., and Karakousis, P.C. (2014). *senX3*-independent contribution of *regX3* to *Mycobacterium tuberculosis* virulence. BMC Microbiol. *14*, 265.

Romero-Rodríguez, A., Maldonado-Carmona, N., Ruiz-Villafán, B., Koirala, N., Rocha, D., and Sánchez, S. (2018). Interplay between carbon, nitrogen and phosphate utilization in the control of secondary metabolite production in *Streptomyces*. Antonie Van Leeuwenhoek *111*, 761–781.

Santos-Beneit, F., Rodríguez-García, A., Franco-Domínguez, E., and Martín, J.F. (2008). Phosphate-dependent regulation of the low- and high-affinity transport systems in the model actinomycete *Streptomyces coelicolor*. Microbiology *154* (Pt 8), 2356–2370.

Seol, E., Sekar, B.S., Raj, S.M., and Park, S. (2016). Co-production of hydrogen and ethanol from glucose by modification of glycolytic pathways in *Escherichia coli*- from Embden-Meyerhof-Parnas pathway to pentose phosphate pathway. Biotechnol. J. *11*, 249–256.

Sola-Landa, A., Moura, R.S., and Martín, J.F. (2003). The two-component PhoR-PhoP system controls both primary metabolism and secondary metabolite biosynthesis in *Streptomyces lividans*. Proc. Natl. Acad. Sci. USA. *100*, 6133–6138.

Sola-Landa, A., Rodríguez-García, A., Franco-Domínguez, E., and Martín, J.F. (2005). Binding of PhoP to promoters of phosphate-regulated genes in *Streptomyces coelicolor*: identification of PHO boxes. Mol. Microbiol. *56*, 1373–1385.

Sola-Landa, A., Rodríguez-García, A., Amin, R., Wohlleben, W., and Martín, J.F. (2013). Competition between the GlnR and PhoP regulators for the *glnA* and *amtB* promoters in *Streptomyces coelicolor*. Nucleic Acids Res. *41*, 1767–1782.

Solans, M., Messuti, M.I., Reiner, G., Boenel, M., Vobis, G., Wall, L.G., and Scervino, J.M. (2019). Exploring the response of Actinobacteria to the presence of phosphorus salts sources: metabolic and co-metabolic processes. J. Basic Microbiol. *59*, 487–495.

Sureka, K., Dey, S., Datta, P., Singh, A.K., Dasgupta, A., Rodrigue, S., Basu, J., and Kundu, M. (2007). Polyphosphate kinase is involved in stress-induced *mprAB-sigE-rel* signalling in *mycobacteria*. Mol. Microbiol. *65*, 261–276.

Vuoristo, K.S., Mars, A.E., Sanders, J.P.M., Eggink, G., and Weusthuis, R.A. (2017). Metabolic engineering of TCA cycle for production of chemicals. Trends Biotechnol. *34*, 191–197.

Vuppada, R.K., Hansen, C.R., Strickland, K.A.P., Kelly, K.M., and McCleary, W.R. (2018). Phosphate signaling through alternate conformations of the PstSCAB phosphate transporter. BMC Microbiol. *18*, 8.

White, D.W., Elliott, S.R., Odean, E., Bemis, L.T., and Tischler, A.D. (2018). *Mycobacterium tuberculosis* Pst/SenX3-RegX3 regulates membrane vesicle production independently of ESX-5 activity. MBio *9*, e00778-18.

Yang, R.J., Liu, X.C., Wen, Y., Song, Y., Chen, Z., and Li, J.L. (2015). The PhoP transcription factor negatively regulates avermectin biosynthesis in *Streptomyces avermitilis*. Appl. Microbiol. Biotechnol. *99*, 10547–10557.

Zhu, C.H., Lu, F.P., He, Y.N., Han, Z.L., and Du, L.X. (2007). Regulation of avilamycin biosynthesis in *Streptomyces viridochromogenes*: effects of glucose, ammonium ion, and inorganic phosphate. Appl. Microbiol. Biotechnol. *73*, 1031–1038.

Supplemental Information

SenX3-RegX3, an Important Two-Component

System, Regulates Strain Growth and Butenyl-spinosyn

Biosynthesis in *Saccharopolyspora pogona*

Jie Rang, Haocheng He, Jianming Chen, Jinjuan Hu, Jianli Tang, Zhudong Liu, Ziyuan Xia, Xuezhi Ding, Youming Zhang, and Liqiu Xia

Supporting Information

Table S1. Oligonucleotides used in this study. Related to Figures 2, 3 and Table 1.

Primers	Sequences (5'-3')	Source/reference
F_{regX3}up	GCT**AAGCTT**TGCCCTTCTTTCCGCACCTA	This work
R_{regX3}up	<u>TCCTTTTTTTCTGCGCGTAATCTGCTGCTTGCAAAC</u>ACGATCAGCACCCTGGTCA	This work
F_{regX3}down	<u>TATTTAAAGATCCACTAGTATGCAGGTCGACGGAT</u>TCGGCTACAAGTTCGAGGGA	This work
R_{regX3}down	GCT**GATATC**ACGACATCCGGGTGATGAAC	This work
F_{apr}	TTTGCAAGCAGCAGATTACG	This work
R_{apr}	ATCCGTCGACCTGCATACTA	This work
F_{regX3}	<u>CGGTTGGTAGGATCCTCTAGAGTCGACCGGCATG</u>CGGGACTGAAAGTGCGGACGG	This work
R_{regX3}	ACG**GAATTC**CGGCATCAAGATTGCCCATT	This work
F_{PermE}	GCT**AAGCTT**CTGGACTTCTAGAGCTAGCC	This work
R_{PermE}	GCATGCCGGTCGACTCTA	This work
F_{RegX3}	TAC**GAATTC**GTGACCAGGGTGCTGATC	This work
R_{RegX3}	CGG**AAGCTT**CTATCCCTCGAACTTGTAGC	This work
F_{SenX3}	GAC**GAATTC**GTGACCGCATTGGGCTGTAC	This work
R_{SenX3}	AGC**AAGCTT**TCACCGGACTCCTCCCGTTT	This work
F_{senX3}	CGGTTCTGCGATGAGCAC	This work
R_{senX3}	GTCAGCATCGTAAGCAAGCC	This work
F_{busA}	GCTCATTCGGTACTGCCCCT	This work
R_{busA}	CGGTCTGCGATTACGAGAAA	This work
$F_{busF-busG}$	ACTAATAACCATCCGGCCAG	This work
$R_{busF-busG}$	CCTGTTGGTCAGGAGTAGGA	This work
$F_{busJ-busI}$	ACTCGTCCAACGACAGCG	This work
$R_{busJ-busI}$	CCGCCGGCTCTACTTTGT	This work

Note: reatricition enzyme sites were bold; overlaping sequences were underlined.

Table S2 qRT-PCR primers used in this study. Related to Figure 3.

Gene ID	Name	Sequence (5'-3')
SP_7030	F_{regX3}	GCCGACCCGCTTGCTTT
	R_{regX3}	AGCTGCTTGCACACATCGGT
SP_3547	F_{busA}	GCAACCTCCCTGGATTACGG
	R_{busA}	ATGAACACGCCGTATCCACC
SP_3548	F_{busF}	ACCAGGTGGACTTCTCGTGC
	R_{busF}	ATCCCGCTGCCTATTTCTCG
SP_3549	F_{busG}	TCCCGCTCAACCTGTTCCTG
	R_{busG}	CTGCTCATCCGGCAAGCAGA
SP_3551	F_{busI}	GTCCTTCCATGCCCTGTTTC
	R_{busI}	AGGCCGTCGATCAGTTCTTT
SP_3552	F_{busJ}	CGCGAGATGTACGCCGAAAC
	R_{busJ}	ACAGGCCGTGCTGGAAGATG
SP_3558	F_{busP}	TGCGACTGCCTGTGGACTTG
	R_{busP}	TGCCTGTTCCTGGGCTTCTC
SP_3559	F_{busQ}	CCCCACGACCATCAATCCAG
	R_{busQ}	GATTCGTCAGCGGCAAAGG

Figure S1
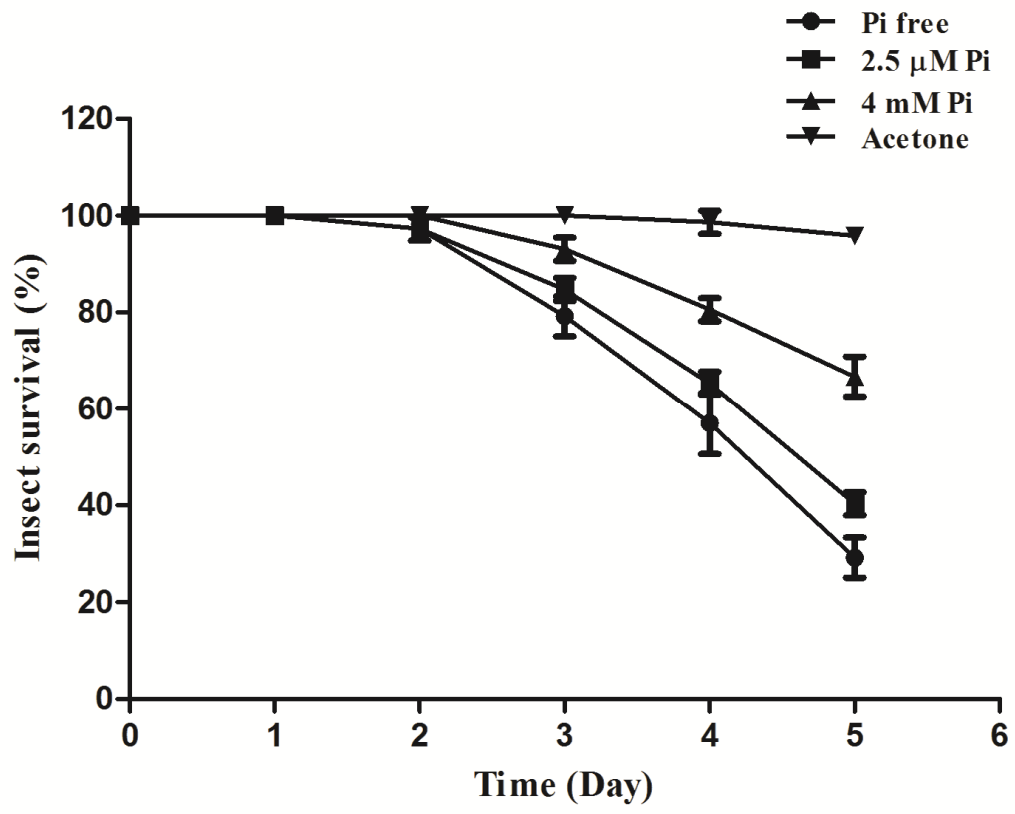
Figure S1. Related Figure 1. Insecticidal changing curve of *Helicoverpa armigera* of *S. pogona* in SFM with different Pi concentration. The acetone was used as the control and observation period was 5 days. From the second day, the insecticidal activity of *S. pogona* in SFM with different Pi concentration have obviously difference. The result showed that the insecticidal activity of the *S. pogona* in SFM without Pi was significantly stronger than in SFM with low and high Pi concentration.

Figure S2

RT: 0.00 - 25.02   NL: 3.98E6
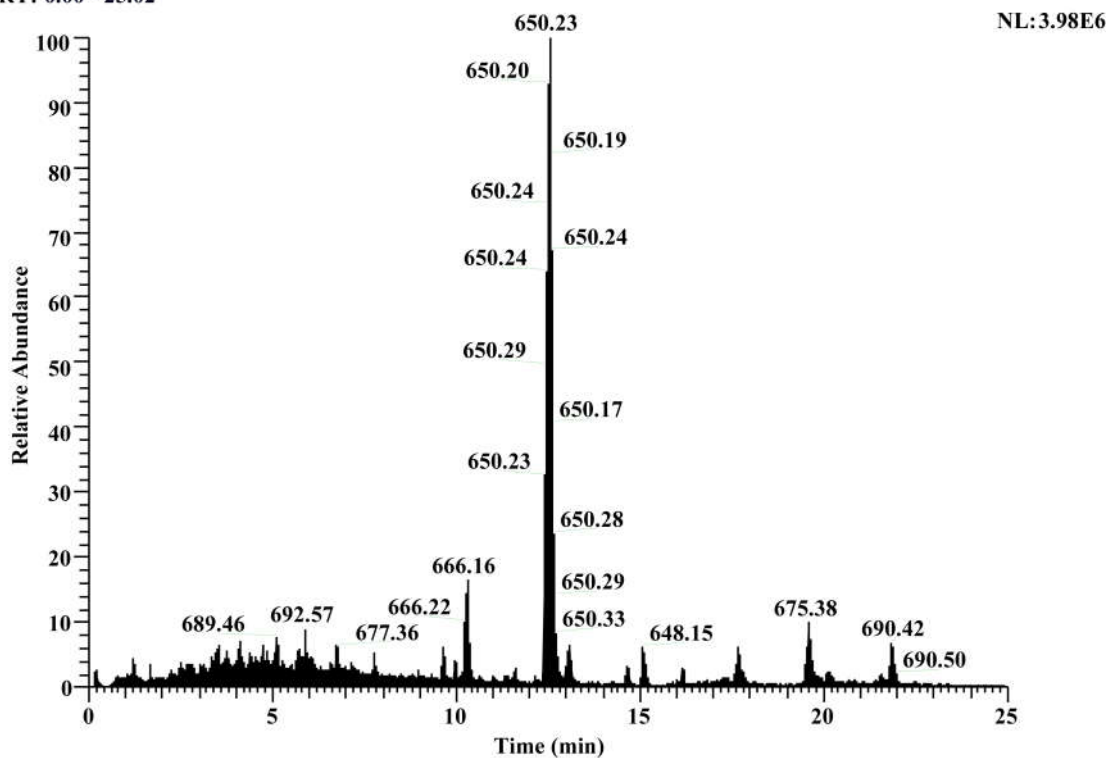
1 #2550   RT: 12.52   AV: 1   NL: 3.52E5
T: ITMS + c ESI d Full ms2 650.20@cid35.00 [165.00-665.00]
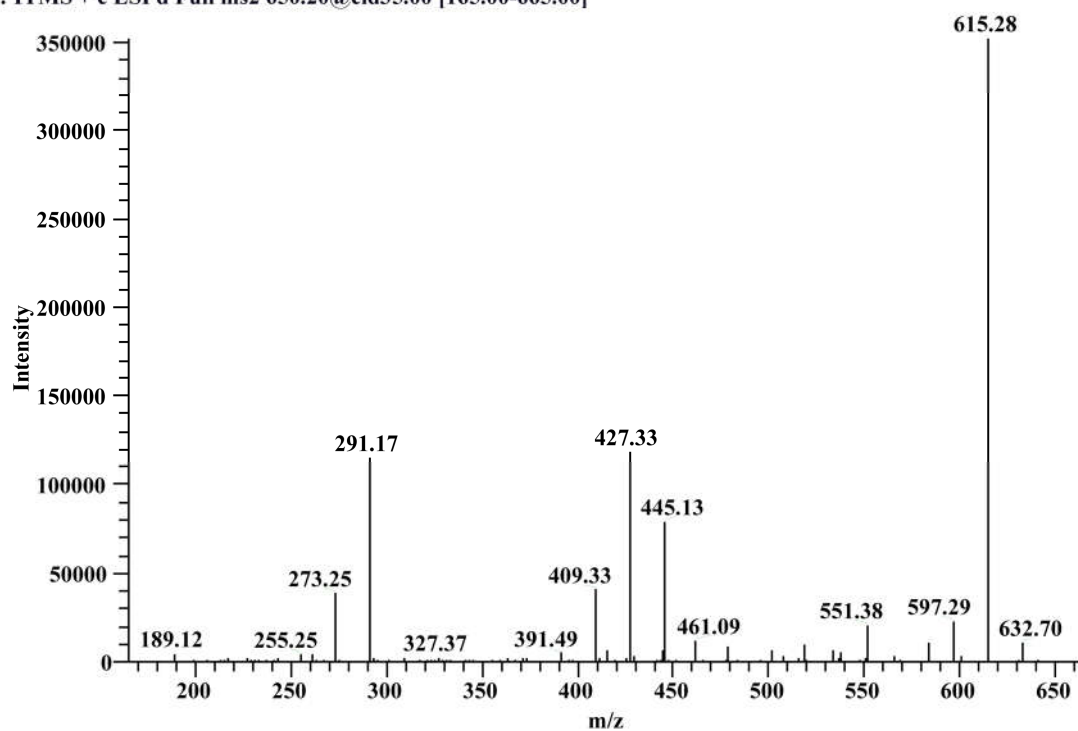
Figure S2. Related to Figure 1 and Figure 3. MS and MS/MS analysis of collected eluents at 10.67 min. The MS identification result showed that the m/z of this substance is 650 $(M + H)^+$. The MS/MS identification result further showed that $(M + H)^+$ ions at m/z = 650 contained a rhamnose ion fragment of 189 molecular mass, which was confirmed as a spinosyn αc.

Figure S3

SFM38871.1 OmpR family response regulator RegX3 Saccharopolyspora antimicrobica
SEG90102.1 OmpR family response regulator RegX3 Saccharopolyspora hirsuta
PTX71889.1 Response regulator RegX3 Saccharopolyspora hirsuta
RKT84914.1 Response regulator RegX3 Saccharopolyspora antimicrobica
SFD89063.1 OmpR family response regulator RegX3 Saccharopolyspora jiangxiensis
RegX3 Saccharopolyspora pogona
PKW13040.1 Response regulator RegX3 Saccharopolyspora spinosa
SDY36943.1 OmpR family response regulator RegX3 Saccharopolyspora shandongensis
SFS46056.1 OmpR family response regulator RegX3 Saccharopolyspora flava
TWF94898.1 Response regulator RegX3 Saccharopolyspora dendranthemae
CAM06127.1 Response regulator Saccharopolyspora erythraea NRRL 2338
PFG99773.1 Response regulator RegX3 Saccharopolyspora erythraea NRRL 2338
AIR99118.1 Sensory transduction protein RegX3 Streptomyces glaucescens
ANZ16941.1 Regulatory protein Streptomyces noursei ATCC 11455
ATZ25387.1 Sensory transduction protein RegX3 Streptomyces lavendulae subsp. lavendulae
AZQ26946.1 Response regulator RegX3 Streptomyces filipinensis
QCX77455.1 Sensory transduction protein RegX3 Streptomyces sp. YIM 121038
RPK61270.1 Sensory transduction protein RegX3 Streptomyces sp. ADI96-02
RUP63891.1 Sensory transduction protein RegX3 Streptomyces sp. NP10
BAG20838.1 Response regulator RegX3 Streptomyces griseus subsp. griseus NBRC 13350
RPK88879.1 Sensory transduction protein RegX3 Streptomyces sp. ADI98-12
CCK29606.1 Sensory transduction protein RegX3 Streptomyces davaonensis JCM 4913
AXE86413.1 Sensory transduction protein RegX3 Streptomyces sp. Go-475
RPK50967.1 Sensory transduction protein RegX3 Streptomyces sp. ADI91-18
RPK82739.1 Sensory transduction protein RegX3 Streptomyces sp. ADI98-10
RPK77541.1 Sensory transduction protein RegX3 Streptomyces sp. ADI97-07
RPK44149.1 Sensory transduction protein RegX3 Streptomyces sp. ADI93-02
AYV26382.1 Sensory transduction protein RegX3 Streptomyces sp. ADI95-16
RPK55204.1 Sensory transduction protein RegX3 Streptomyces sp. ADI96-15
RII09473.1 Sensory transduction protein RegX3 Streptomyces sp. YIM 130001
RPK48076.1 Sensory transduction protein RegX3 Streptomyces sp. ADI92-24
AYG80473.1 Transcriptional regulatory protein PhoP Streptomyces hundungensis
ODA72832.1 Transcriptional regulatory protein PhoP Streptomyces sp. AVP053U2
PSK56146.1 Transcriptional regulatory protein PhoP Streptomyces sp. 111WW2
PPS89399.1 Transcriptional regulatory protein PhoP Streptomyces sp. MH60
OAH13514.1 Transcriptional regulatory protein PhoP Streptomyces jeddahensis
SPF05876.1 Transcriptional regulatory protein PhoP Streptomyces sp. MA5143a
OSY49752.1 Transcriptional regulatory protein PhoP Streptomyces fradiae ATCC 10745 DSM 40063
AOT61017.1 Transcriptional regulatory protein PhoP Streptomyces rubrolavendulae
RPK91264.1 Transcriptional regulatory protein PhoP Streptomyces sp. ADI98-10
RPK43662.1 Transcriptional regulatory protein PhoP Streptomyces sp. ADI92-24
QHY96859.1 Sensory transduction protein Streptomyces sp. S4.7
RPK72656.1 Sensory transduction protein Streptomyces sp. ADI95-17
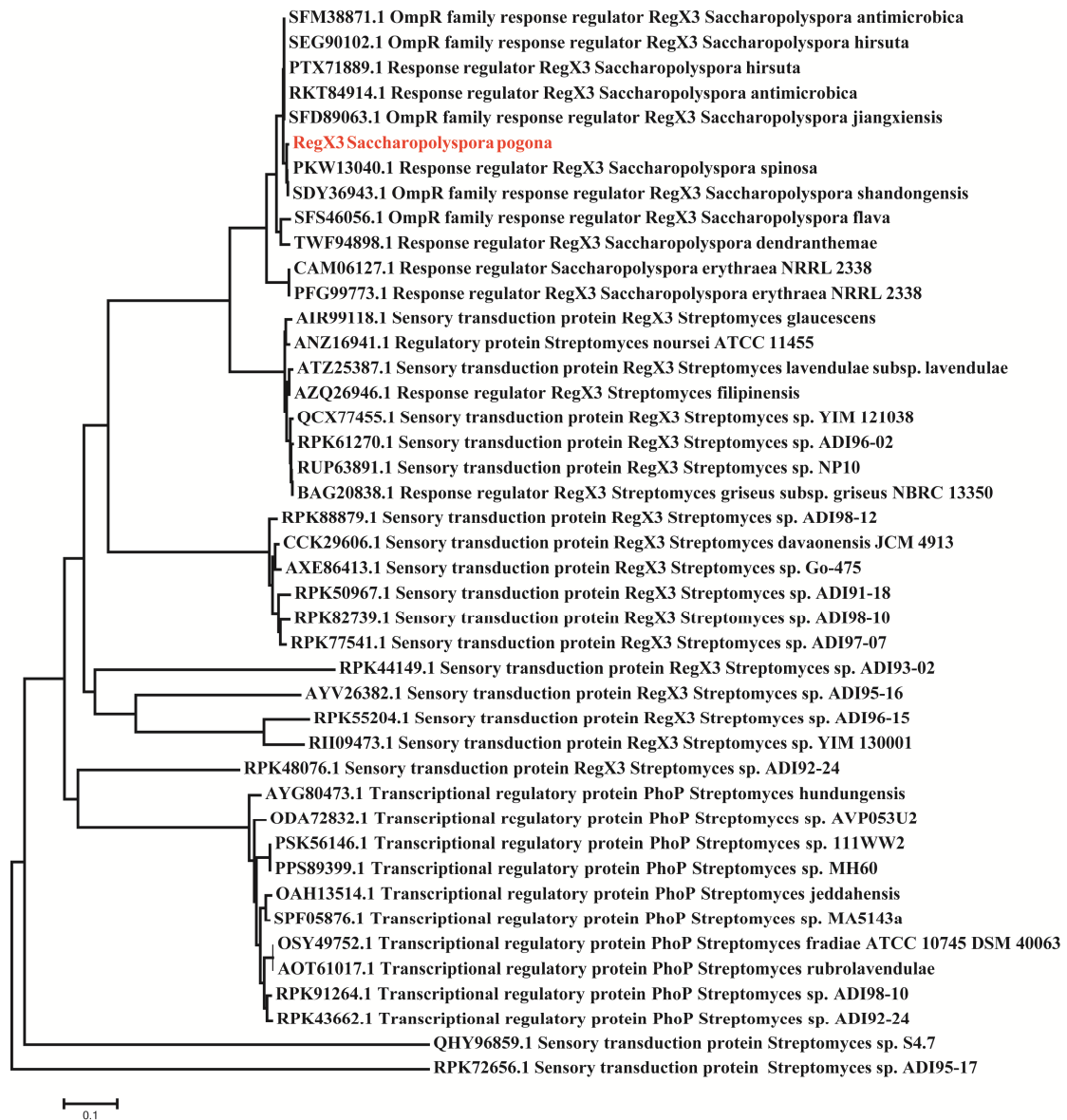
0.1

Figure S3. Related to Figure 1. Phylogenetic tree analysis of RegX3 (red). MEGA

5.02 was used to construct the tree by the neighbor-joining method based on RegX3
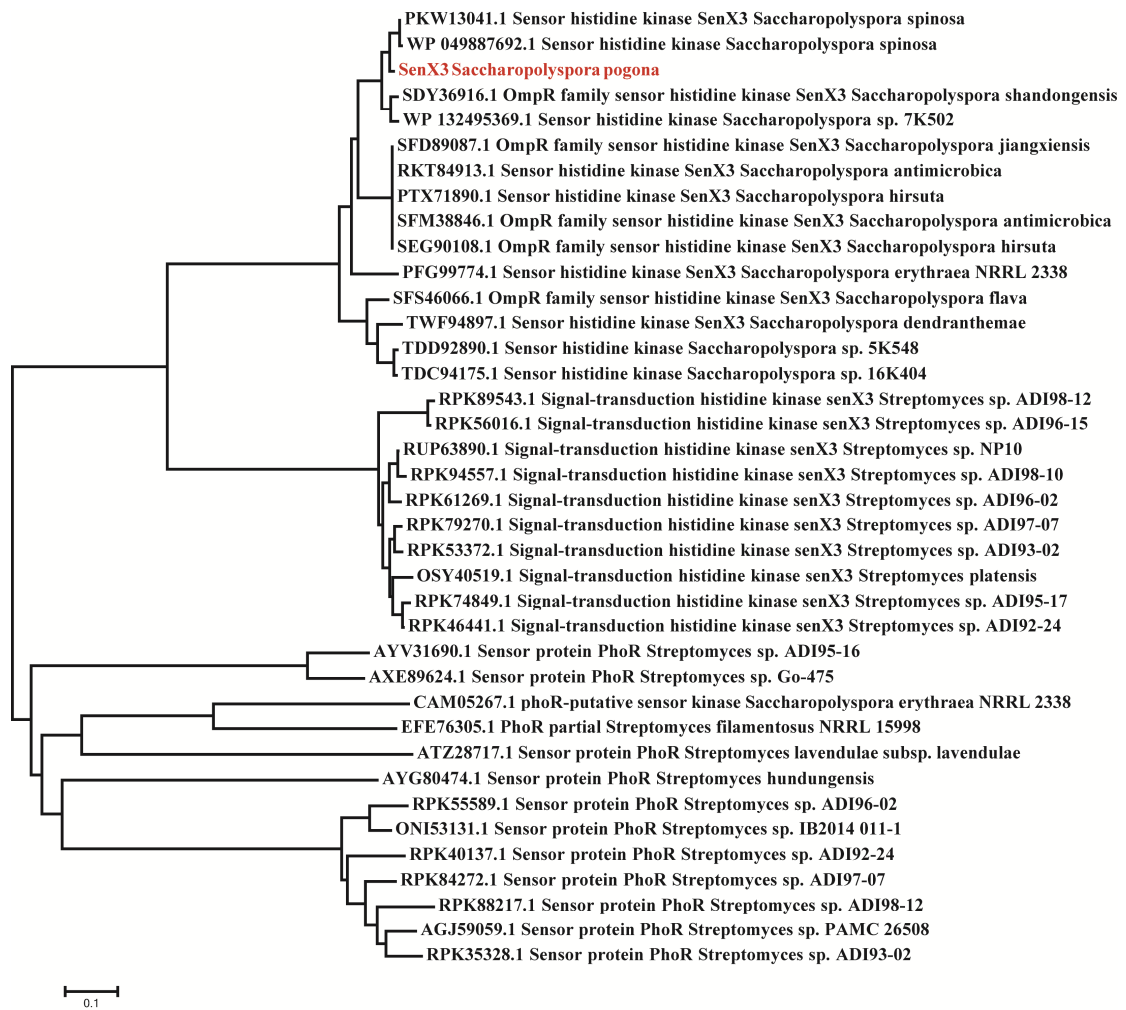
Protein sequence.

Figure S4

PKW13041.1 Sensor histidine kinase SenX3 Saccharopolyspora spinosa
WP 049887692.1 Sensor histidine kinase Saccharopolyspora spinosa
SenX3 Saccharopolyspora pogona
SDY36916.1 OmpR family sensor histidine kinase SenX3 Saccharopolyspora shandongensis
WP 132495369.1 Sensor histidine kinase Saccharopolyspora sp. 7K502
SFD89087.1 OmpR family sensor histidine kinase SenX3 Saccharopolyspora jiangxiensis
RKT84913.1 Sensor histidine kinase SenX3 Saccharopolyspora antimicrobica
PTX71890.1 Sensor histidine kinase SenX3 Saccharopolyspora hirsuta
SFM38846.1 OmpR family sensor histidine kinase SenX3 Saccharopolyspora antimicrobica
SEG90108.1 OmpR family sensor histidine kinase SenX3 Saccharopolyspora hirsuta
PFG99774.1 Sensor histidine kinase SenX3 Saccharopolyspora erythraea NRRL 2338
SFS46066.1 OmpR family sensor histidine kinase SenX3 Saccharopolyspora flava
TWF94897.1 Sensor histidine kinase SenX3 Saccharopolyspora dendranthemae
TDD92890.1 Sensor histidine kinase Saccharopolyspora sp. 5K548
TDC94175.1 Sensor histidine kinase Saccharopolyspora sp. 16K404
RPK89543.1 Signal-transduction histidine kinase senX3 Streptomyces sp. ADI98-12
RPK56016.1 Signal-transduction histidine kinase senX3 Streptomyces sp. ADI96-15
RUP63890.1 Signal-transduction histidine kinase senX3 Streptomyces sp. NP10
RPK94557.1 Signal-transduction histidine kinase senX3 Streptomyces sp. ADI98-10
RPK61269.1 Signal-transduction histidine kinase senX3 Streptomyces sp. ADI96-02
RPK79270.1 Signal-transduction histidine kinase senX3 Streptomyces sp. ADI97-07
RPK53372.1 Signal-transduction histidine kinase senX3 Streptomyces sp. ADI93-02
OSY40519.1 Signal-transduction histidine kinase senX3 Streptomyces platensis
RPK74849.1 Signal-transduction histidine kinase senX3 Streptomyces sp. ADI95-17
RPK46441.1 Signal-transduction histidine kinase senX3 Streptomyces sp. ADI92-24
AYV31690.1 Sensor protein PhoR Streptomyces sp. ADI95-16
AXE89624.1 Sensor protein PhoR Streptomyces sp. Go-475
CAM05267.1 phoR-putative sensor kinase Saccharopolyspora erythraea NRRL 2338
EFE76305.1 PhoR partial Streptomyces filamentosus NRRL 15998
ATZ28717.1 Sensor protein PhoR Streptomyces lavendulae subsp. lavendulae
AYG80474.1 Sensor protein PhoR Streptomyces hundungensis
RPK55589.1 Sensor protein PhoR Streptomyces sp. ADI96-02
ONI53131.1 Sensor protein PhoR Streptomyces sp. IB2014 011-1
RPK40137.1 Sensor protein PhoR Streptomyces sp. ADI92-24
RPK84272.1 Sensor protein PhoR Streptomyces sp. ADI97-07
RPK88217.1 Sensor protein PhoR Streptomyces sp. ADI98-12
AGJ59059.1 Sensor protein PhoR Streptomyces sp. PAMC 26508
RPK35328.1 Sensor protein PhoR Streptomyces sp. ADI93-02

0.1

Figure S4. Related to Figure 1. Phylogenetic tree analysis of SenX3 (red). MEGA

5.02 was used to construct the tree by the neighbor-joining method based on SenX3
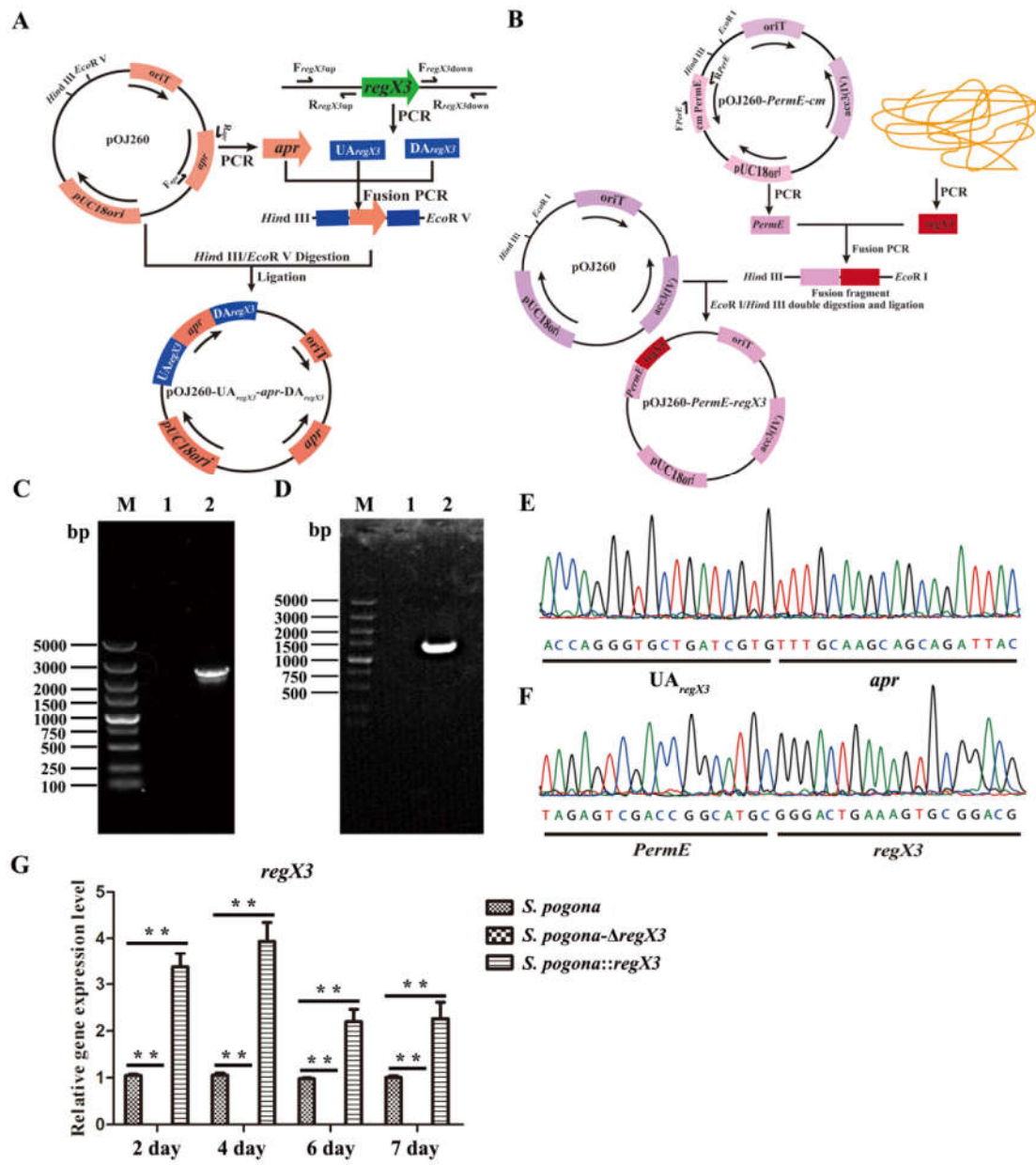
Protein sequence.

Figure S5

Figure S5. Related to Figures 2, 3, 4, 5, 6 and Table 1. Deletion and overexpression of *regX3*.

(A) Schematic diagrams of the *S. pogona*-Δ*regX3* mutant. (B) Schematic diagrams of the *S. pogona*::*regX3* mutant. (C) PCR identification of the *S. pogona*-Δ*regX3* mutant. The wild-type *S. pogona* genomic DNA was used as the control. Lane M, DL5000 DNA marker; lane 1, control; lane 2, *S. pogona*-Δ*regX3* mutant. The tested transformant showed 2.8-kb PCR amplicon, whereas control showed no band in the same place. (D) PCR identification of the *S. pogona*::*regX3* mutant. The wild-type *S. pogona* genomic DNA was used as the control. Lane M, DL5000 DNA marker; lane 1, control; lane 2, *S. pogona*::*regX3* mutant. The tested transformant showed 1.2-kb PCR amplicon, whereas control showed no band in the same place. (E) The sequencing of the *S. pogona*-Δ*regX* mutant PCR amplicon. (F) The sequencing of the *S. pogona*::*regX3* mutant PCR amplicon. (G) The transcriptional level analysis of *regX3* in *S. pogona* and its derivative. The cells of the different strains were inoculated into SFM and cultured at 30℃ for 2 days, 4 days, 6 days and 8 days. Total RNA was then isolated and used for qRT-PCR assays. The control strain was wild-type *S. pogona*. 16S rRNA served as the normalization control.

Figure S6
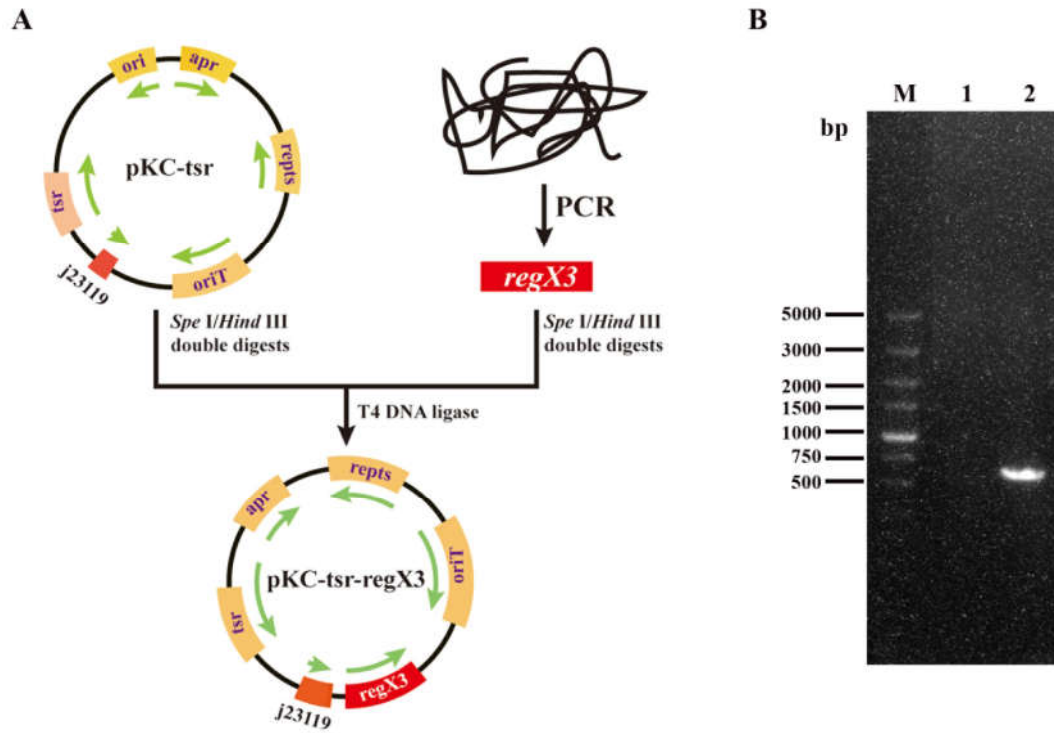
Figure S6. Related to Figures 2, 3F, 4 and Table 1. Complementation of *regX3* in the *S. pogona*-Δ*regX3* mutant.

(A) Schematic diagrams of the complemented strain *S. pogona*-Δ*regX3*::*regX3*. (B) PCR identification of the complemented strain *S. pogona*-Δ*regX3*::*regX3*. The wild-type *S. pogona* genomic DNA was used as the control. Lane M, DL5000 DNA marker; lane 1, control (*S. pogona*-Δ*regX3*); lane 2, complemented strain *S. pogona*-Δ*regX3*::*regX3*. The tested transformant showed 681-bp PCR amplicon, whereas control showed no band in the same place.

Figure S7
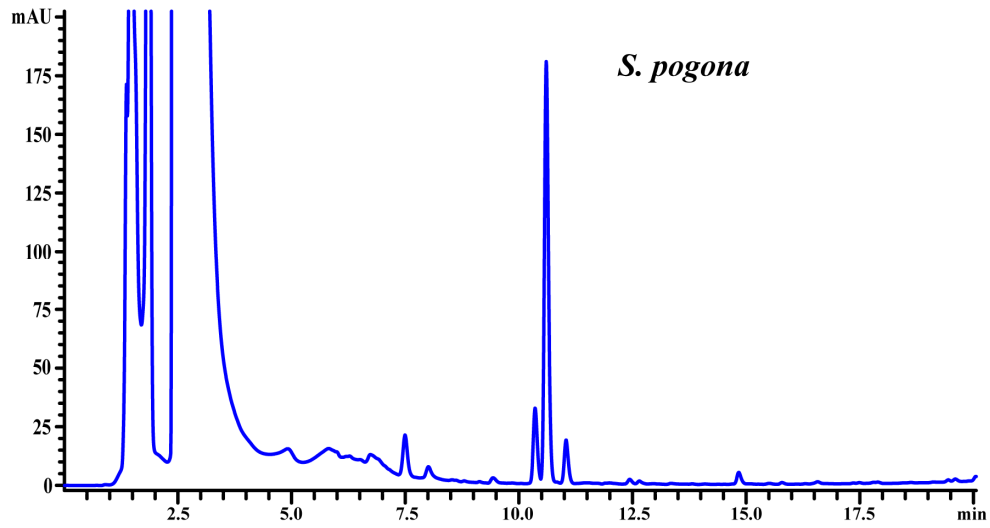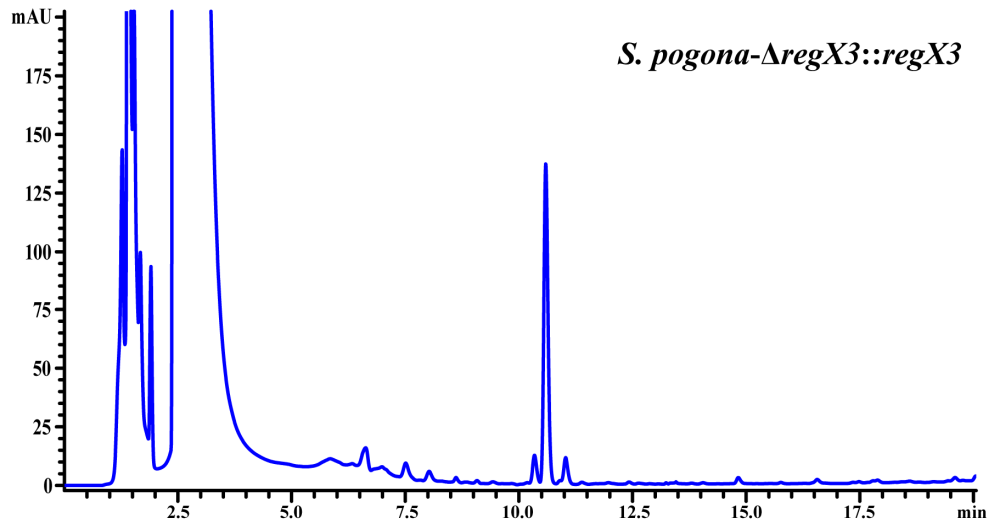
Figure S7. Related to Figure 2 and Table 1. Butenyl-spinosyn production analysis of complemented strain *S. pogona*-Δ*regX3*::*regX3*

Figure S8
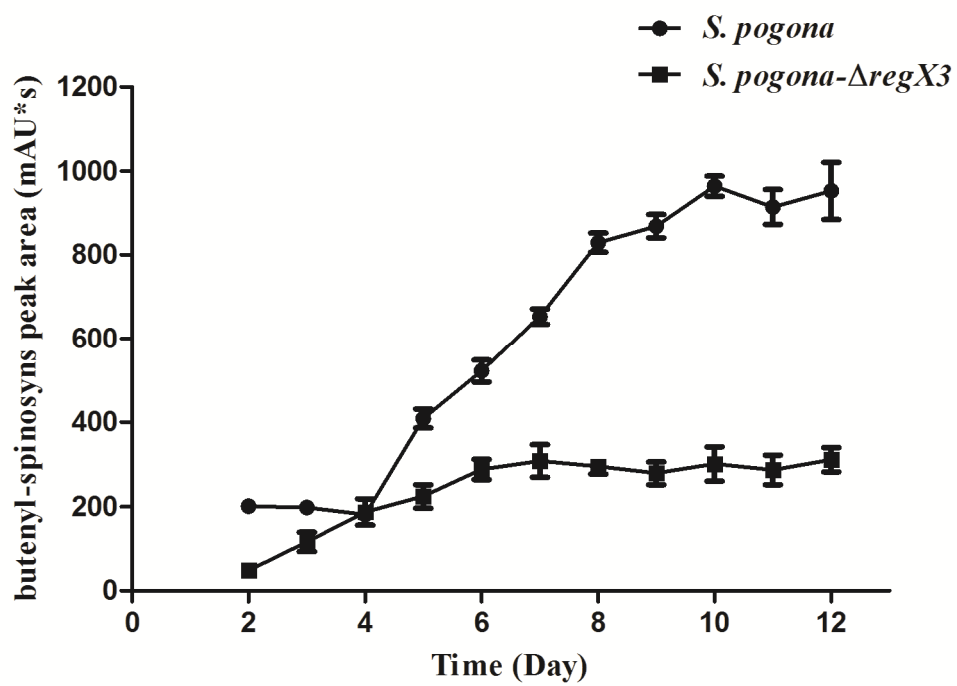
Figure S8. Related to Figures 5, 6 and Table 1. Butenyl-spinosyn yield curve of mutant *S. pogona*-Δ*regX3* and wild-type *S. pogona*.
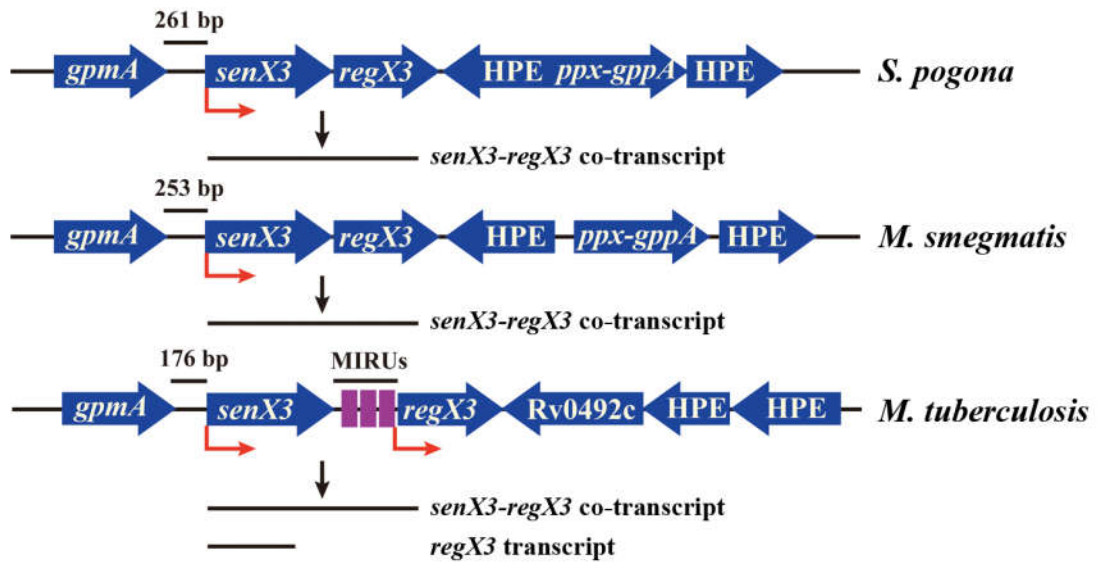
Figure S9

Figure S9. Related to Figure 2. Arrangement of the *senX3-regX3* system and the adjacent genes in *S. pogona*, *M. semgmatis* and *M. tuberculosis*. The organization of *senX3-regX3* and the adjacent genes *gpmA* and *ppx-gppA* is the same in *S. pogona* as in the homologous region in *M. semgmatis,* suggesting that the *senX3-regX3* system of *S. pogona* may exhibit similar transcription patterns and biological functions to that of *M. semgmatis*.

Transparent Methods

Bacterial strains, plasmids, and media

Escherichia coli (*E. coli*) DH5α was used to construct the recombinant plasmids (Yoshida and Sato, 2009). *E. coli* BL21 was used as the host for heterologous protein production (Wu et al., 2019). All *E. coli* strains were grown at 37 °C in Luria-Bertani broth. The complete synthetic medium (CSM; per liter: 10 g of glucose, 45 g of trypticase soy broth, 9 g of yeast extract, and 2.2 g of $MgSO_4 \cdot 7H_2O$) was used for *S. pogona* and its derivatives activation. For butenyl-spinosyn fermentation and other phenotypic analysis, synthetic fermentation medium (SFM; per liter: 1 g of KNO_3, 0.01 g of $FeSO_4 \cdot 7H_2O$, 0.5 g of $K_2HPO_4 \cdot 3H_2O$, 0.5 g of $MgSO_4 \cdot 7H_2O$, 20 g of glucose, 4 g of yeast extract, 4 g of tryptone; pH of 7.2) was employed. SFM with different concentrations of $K_2HPO_4 \cdot 3H_2O$ (0, 2.5×10^{-3} and 4 μm) were used to analyse the effects of phosphate on the growth development and butenyl-spinosyn biosynthesis of *S. pogona*. The R5 medium (per liter: 103 g of sucrose, 10 g of glucose, 0.1 g of casein hydrolysate, 5 g of yeast extract, 5.73 g of TES, 0.25 g of K_2SO_4, 10.12 g of $MgCl_2 \cdot 6H_2O$, 2 mL of microelement solution, and 15 g of agar) was used for *S. pogona* protoplast transformation. R5 medium (100 mL) was supplemented with 1 mL KH_2PO_4 (0.5%), 10 mL $CaCl_2 \cdot 2H_2O$ (3.68%), and 10 mL TES buffer (5.73%, pH7.2) before use. If necessary, 50 μg/ml apramycin (Apra) was added into the above media.

Determination of growth kinetics and butenyl-spinosyn production

Optical density at 600 nm (OD_{600}) was used to determine the cell concentration. Cells

were collected every 12 h during fermentation for growth curve measurements by UV scanning and a certain dilution ratio was chosen to ensure that the measured value ranged from 0.2 to 0.8.

The cells were collected in SFM at 10th day to determine the butenyl-spinosyn production using HPLC 1290 system. The sample processing and testing methods as described previously with slight modification (Li et al., 2018). The fermentation broth was mixed with acetone at a 1:1 volumetric ratio for 48 h. Cultures were centrifuged at 9,000 g for 15 min, and the supernatants were filtered through 0.22 μm Millipore filters. After filtration, a 10 μL sample was loaded onto a C18 column (AQ12S05-1546WT, YMC, Kyoto, Japan) and gradient eluted with the elution buffer at 1.0 mL/min. The elution buffer composed of solvent A (water) and solvent B (acetonitrile). Each chromatographic separation lasted 20 min with the following gradient: 60% B (2.5 min hold) ramped to a final mobile phase concentration of 100% B for 10.5 min (3 min hold). The detection wavelength was set at 250 nm during the analysis. MS analysis was performed using an Thermo LTQ XL Ion Trap mass spectrometer in positive electrospray ionization mode (Thermo Scientific, USA). The 15 μL sample (Chromatographic peak collected) was loaded onto a C18 column (LAGV-25005-102130, Thermo Scientific, USA) and gradient eluted with the elution buffer at 300 μL/min. The elution buffer composed of solvent A (water, 0.1% formic acid, v/v) and solvent B (methanol, 0.1% formic acid, v/v). Each chromatographic separation lasted 20 min with the following gradient: 50% B (2 min hold) ramped to a final mobile phase concentration of 100% B for 10 min (5 min hold). The mass

analyzer was scanned over a mass range of 80 to 800 m/z. Data analysis and instrument operations were performed under Xcaliber software control. The *Helicoverpa armigera* (*H. armigera*) bioassay was used to verify whether the collected chromatographic peak had insecticidal activity as described previously (Li et al., 2018).

regX3 deletion, complementation and overexpression

Targeted gene deletion mediated by homologous recombination was used to generate a *regX3* null mutant. With *S. pogona* genomic DNA as template, a 1.5-kb fragment upstream (UA$_{regX3}$) of *regX3* was amplified with primers F$_{regX3up}$ and R$_{regX3up}$, and a 1.5-kb fragment downstream (DA$_{regX3}$) of *regX3* was amplified with primers F$_{regX3down}$ and R$_{regX3down}$. With pOJ260 plasmid DNA as template, 1.3-kb apramycin resistance gene (*apr*) was amplified with primers F$_{apr}$/R$_{apr}$. The 5'-end of R$_{regX3up}$ and F$_{regX3down}$ have a 35-nt overlapping sequence respectively, allowing the joining of UA$_{regX3}$, *apr* and DA$_{regX3}$ in a subsequent fusion PCR reaction. The resulting 4.3 kb fusion fragment was digested with *Hin*d III and *Eco*R V and cloned into the corresponding restriction sites of pOJ260, yielding pOJ260-UA$_{regX3}$-*apr*-DA$_{regX3}$. Then, this plasmid was transformed into *S. pogona* by protoplast transformation. Transformants were selected directly on R5 plates containing 50 μg/ml apramycin. Since pOJ-260 is a suicide plasmid, it cannot be replicated in *S. pogona* and will eventually be lost as the strain grows. Therefore, the chromosome structure at the *regX3* locus of several Apra^R colonies was analysed by PCR using primers F$_{regX3up}$/R$_{apr}$ and sequencing (Sangon Biotech, Shanghai), and the mutant that was successfully verified was named *S.*

pogona-Δ*regX3*.

For *regX3* overexpression, plasmid pOJ260-*cm-PermE* was used to amplify strong constitutive promoter *PermE* with primers F$_{PermE}$ and R$_{PermE}$. *S. pogona* NRRL 30141 as the template for *regX3* amplification by PCR and the primers was F$_{regX3}$ and R$_{regX3}$. The 5'-end of F$_{regX3}$ have a 35-nt overlapping sequence, allowing the joining of *PermE* and *regX3* in a subsequent fusion PCR reaction. The resulting 1.2 kb fusion fragment was digested with *Hin*d III and *Eco*R I and cloned into the corresponding restriction sites of pOJ260, yielding pOJ260-*PermE-regX3*. Then, this plasmid was transformed into *S. pogona* by protoplast transformation. Transformants were selected directly on R5 plates containing 50 µg/mL apramycin. The chromosome structure at the *regX3* locus of several Apra[R] colonies was analysed by PCR using primers F$_{RegX3}$/R$_{RegX3}$, and the mutant that was successfully verified was named *S. pogona*::*regX3*.

For *regX3* complementation, the *regX3* was digested with *Spe* I and *Hin*d III, and cloned into the corresponding restriction sites of pKC-*tsr*, yielding pKC-*tsr-regX3*. Then, this plasmid was transformed into *S. pogona*-Δ*regX3* mutant by protoplast transformation. Transformants were selected directly on R5 plates containing 15 µg/mL thiostrepton. The chromosome structure at the *regX3* locus of several Tsr[R] colonies was analysed by PCR using primers F$_{RegX3}$/R$_{RegX3}$, and the mutant that was successfully verified was named *S. pogona*-Δ*regX3*::*regX3*.

Polyphosphate extraction and determination

DAPI (4',6-diamidino-2-phenylindole) was used to compare the difference of

Polyphosphate (polyP) in mutants and original strain (Du et al., 2019). PolyP was extracted from *S. pogona* and its derivatives as described previously with slight modifications. Bacteria of early and stationary phase in 50 ml of SFM were pelleted (9,000 g for 15 min), and then resuspended in 1.0 ml of HEPES (20 mM, pH = 7.0) and stored at 80°C until polyP was extracted. The processed samples (300 μL) were transferred to new 1.5-ml tubes containing 600 μL of HEPES. During the measurement, 100 μl DAPI solution (100 μM) was added to the experimental group and 100 μl H_2O was used to replace DAPI in the control group. The binding of DAPI to polyP causes a shift in absorbance from 414 nm to 550 nm. Absorbance at 414 nm and 550 nm was measured using the Microplate Reader (Thermo Scientific, USA). All assays were performed in triplicate in order to calculate standard deviation.

Cultivation profile analysis of the *S. pogona* and its derivatives

Cells were collected every 24 h to determine butenyl-spinosyn production by using a HPLC system (1290, Agilent, USA). Cells were collected every 12 h during fermentation for growth curve measurements by UV scanning and a certain dilution ratio was chosen to ensure that the measured value ranged from 0.2 to 0.8. Supernatants were collected every 24 h during fermentation to determine the glucose concentration until the glucose was used up. The assay method as described previously (Gallo et al., 2010), which was analysed by a LC system (ÄKTA Purifier10, GE Healthcare, MA, USA) equipped with an AMINEX HPX-87 H column (Bio-Rad Laboratories, Hercules, CA) and detected at 210 nm. All of the experiments were performed in triplicate.

Heterologous expression and purification of RegX3 and SenX3

To performed the heterologous expression of *regX3* and *senX3*, the 681-bp *regX3* and 1245-bp *senX3* were obtained using the primer pairs F_{RegX3}/R_{RegX3}, F_{SegX3}/R_{SegX3} and *S. pogona* genome as template. The PCR-amplified product was digested with *Eco*R I and *Hin*d III, and then cloned into the corresponding restriction sites of pET28a, which contained the His-tag, yielding pET28a-*regX3* and pET28a-*senX3*, respectively. The constructed plasmids were introduced into *E. coli* BL21, and induced by 0.5 mM IPTG at 16 °C for 20-24 h. The recombinant His_6-tagged RegX3 and His_6-tagged SenX3 were extracted and purified on Ni^{2+}-NTA Sefinosex column (Sangon Biotech, Shanghai). The quality of the purified proteins was estimated by polyacrylamide gel electrophoresis (SDS-PAGE) and stored at 4 °C.

Electrophoretic mobility shift assays (EMSAs)

The EMSAs were performed according to the manufacturer's instructions (DIG Gel Shift Kit, second generation, Roche). DNA fragments used for EMSAs analysis were amplified by PCR with the primers listed in Table S1. 10 μL His_6RegX3 was phosphorylated by 2 μM His_6SenX3 in phosphorylation buffer (10 mM $MgCl_2$, 50 mM KCl, 25 mM Tris-HCl, pH 8.0, 0.5 mM EDTA, 10 mM ATP, 5% glycerol) for 20 to 30 min at room temperature. During the EMSAs, the DNA fragment was incubated individually with varying quantities of RegX3-P at 25 °C for 30 min in phosphorylation buffer. As a positive control, the same reaction was performed in the presence of *senX3* promoter. After incubation, protein-bound and free DNAs were separated by electrophoresis on 5.0 % native polyacrylamide gels with

0.5×Tris-borate-EDTA (TBE) buffer (44.5 mM Tris-HCl, 44.5 mM boric acid, and 1 mM EDTA, pH 8.0) as running buffer at 100 V and 4 °C. After separation, the gel was scanned and analyzed by Syngene G (USA).

Whole proteins extraction, preparation and LC-MS/MS analysis of the whole proteins

The cells of *S. pogona*-Δ*regX3* mutant and the original strain were harvested (9,000 g, 10 min, 4 °C) after 6 days of culture, washed four times by resuspending the cell pellet in 20 mL of fresh PBS (10 mM, pH 7.8, pre-chilled at 4 °C), and quickly frozen in liquid nitrogen. Protein extraction and 2D LC-MS/MS analysis were performed as described previously with slight modification (Yang et al., 2014). Each protein extract (300 μg) was reduced with 500 mM dithiothreitol (DTT) at room temperature for 60 min and then alkylated with 500 mM iodoacetamide at room temperature in the dark for 60 min. Excess iodoacetamide was quenched with 15 mM DTT for 15 min at room temperature. The sample solutions were then incubated overnight with trypsin at a trypsin/protein ratio of 1:50 (w/w) at 37 °C. Tryptic peptides were desalted and concentrated on an Oasis HLB sample cartridge column (Waters Corporation, MA, USA). Subsequently, the samples were labeled with an iTraq reagent in accordance with the manufacturer's protocol (ABSciex, Framingham, MA, USA) and then lyophilized for further 2D online LC-MS analysis.

2D chromatography was conducted on an Eksigent nano LC-Ultra™1D System (AB SCIEX, Concord, ON). The lyophilized SCX fractions were re-dissolved in 2% acetonitrile and 0.1% formic acid and then loaded on a ChromXP C18 (3 μm, 120 Å)

nanoLC trap column. Online trapping and the desalting were performed at 2 µL/min for 10 min with 100% solvent A. The solvents were composed of water/acetonitrile/formic acid (A, 98%/2%/0.1%; B, 2%/98%/0.1%). An elution gradient of 5%–38% acetonitrile (0.1% formic acid) in 70 min gradient was then employed on an analytical column (75 µm × 15 cm C18, 3 µm, 120 Å, ChromXP Eksigent). LC-MS/MS analysis was performed using a TripleTOF 5600 System (SCIEX, Concord, ON) fitted with a Nanospray III source. Data were acquired at an ion spray voltage of 2.4 kV, a curtain gas of 30 PSI, a nebulizer gas of 5 PSI, and an interface heater temperature of 150 °C. MS was operated with TOF-MS scans. For information dependent acquisition (IDA), the survey scans were acquired in 250 ms, and up to 30 product ion scans (80 ms) were collected if the threshold of 260 counts was exceeded and with a +2 to +5 charge state. Rolling collision energy setting was applied to all precursor ions for collision-induced dissociation. Dynamic exclusion was set to 16 s.

Protein Identification and bioinformatics analysis

LC-MS/MS data were analyzed for protein identification and quantification using the ProteinPilot software v.4.5 (Sciex Inc., USA). The utilized protein database was the protein sequence set of all *Saccharopolyspora* strains. False discovery rate (FDR) was estimated via a reverse database strategy, and only proteins below the threshold of 1% of FDR were further considered. The differential abundant proteins (DAPs) were defined in the iTraq experiment on the basis of the following criteria: unique peptides ≥ 1, P value < 0.05, and fold change > 1.33 or < 0.75. Only proteins present in all the

replicate samples were considered for subsequent analysis. The DAPs were annotated

using the GO database (http://www.geneontology.org/), and proteins were classified

based on functional annotations using the GO terms for cellular components,

biological processes, and molecular functions. The metabolic pathway analysis of

DAPs was conducted using the KEGG database (http://www.genome.jp/kegg/).

Determination of intracellular metabolites associated with energy metabolism by

LC-MS/MS

For targeted metabolomic analysis, samples were collected at 6 days, and the sample

treatment methods used were as described by Yang et al with some modifications

(Yang et al., 2018). 10 mL of culture broth were collected and centrifuged, the

samples were transferred to EP tubes and mixed with 400 μL of methanol/acetonitrile

(1:1, v/v). The tubes were vortexed for 30 s, incubated for 10 min at -20 °C, and then

centrifuged at 14,000 g for 15 min at 4 °C. The supernatants were collected and dried

with nitrogen, and then, the lyophilized powder was stored at -80 °C prior to analysis.

A targeted metabolites analysis was performed using an LC-MS/MS system. The

dried metabolites were dissolved in 100 μL of acetonitrile/H_2O (1:1, v/v) and

centrifuged (13,000 g) for 15 min. Electrospray ionization was conducted with an

Agilent 1290 Infinity chromatography system and AB Sciex QTRAP 5500 mass

spectrometer. NH_4COOH (15 mM) and acetonitrile were used as mobile phases A and

B, respectively. A binary solvent gradient was used as follows: A, NH_4COOH; B, 0-18

min at 90% to 40% acetonitrile; 18-18.1 min at 40% to 90% acetonitrile; and 18.1-23

min at 90% acetonitrile. The LCMS/MS was operated in the negative mode under the

following conditions: source temperature, 450 °C; ion source gas 1, 45; ion source gas 2, 45; curtain gas, 30; and ion spray voltage floating (ISVF), -4500 V.

RNA isolation, cDNA synthesis and quantitative reverse transcription PCR

Total RNAs of the *S. pogona* and its derivatives were separately isolated by using TRIzol Reagent (Invitrogen). RNA concentration and purity were determined by measuring the ratio of OD_{260} nm to OD_{280} nm. DNase treatment and cDNA synthesis were carried out by RNase-free DNase 1 (Invitrogen) and a High-capacity cDNA Archive kit (Fermentas) according to each manufacturer's instructions. The real time qPCR amplification was performed by using Power SYBRR Green PCR Master Mix (Applied Biosystems), as previously described (Yang et al., 2014). The sequences of the primers used in qRT-PCR were developed with Primer Premier 5.0 and listed in Table S1. Transcript generated from the 16S rRNA gene was used for normalization. Results were shown as the means of four replicate experiments.

Statistical analysis

All data in this study were stated as means ± standard error of mean (SEM), and analysis by Student't t-test, with $*p < 0.05$, $**p < 0.01$, ns, no significant.

References

Du, Y.L., Han, Z.L., Wang, X.Y., Wan, C.S. (2019) A fluorometric method for direct detection of inorganic polyphosphate in enterohemorrhagic *Escherichia coli* O157:H7. Nan Fang Yi Ke Da Xue Xue Bao. 39(3): 344-350.

Gallo, G., Alduina, R., Renzone, G., Thykaer, J., Bianco, L., Eliasson-Lantz, A., Scaloni, A, Puglia, A.M. (2010) Differential proteomic analysis highlights metabolic

strategies associated with balhimycin production in *Amycolatopsis balhimycina* chemostat cultivations. Microb. Cell Fact. 9: 95-95.

Li, L., Rang, J., He, H.C., He, S.Y., Liu, Z.D., Tang, J.L., Xiao, J., He, L., Hu, S.B., Yu, Z.Q., Ding, X.Z., Xia, L.Q. (2018) Impact on strain growth and butenyl-spinosyn biosynthesis by overexpression of polynucleotide phosphorylase gene in *Saccharopolyspora pogona*. Appl. Microbiol. Biotechnol. 102(18): 8011-8021.

Wu, H., Chu, Z.L., Zhang, W.X., Zhang, C., Ni, J.S., Fang, H.S., Chen, Y.H., Wang, Y.S., Zhang, L.X., Zhang, B.C.. (2019) Transcriptome-guided target identification of the TetR-like regulator SACE_5754 and engineered overproduction of erythromycin in *Saccharopolyspora erythraea*. J. Biol. Eng. 13:11.

Yang, J., Fu, M.M., Ji, C., Huang, Y.C., Wu, Y.R. (2018) Maize oxalyl-CoA decarboxylase1 degrades oxalate and affects the seed metabolome and nutritional quality. Plant Cell. 30(10): 2447-2462.

Yang, Q., Ding, X.Z., Liu, X.M., Liu, S., Sun, Y.J., Yu, Z.Q., Hu, S.B., Rang, J., He, H., He, L., Xia, L.Q. (2014) Differential proteomic profiling reveals regulatory proteins and novel links between primary metabolism and spinosad production in *Saccharopolyspora spinosa*. Microb. Cell. Fact. 13(1): 27.

Yoshida, N., Sato, M. (2009) Plasmid uptake by bacteria: a comparison of methods and efficiencies. Appl. Microbiol. Biotechnol. 83(5): 791-798.